PRODUCTION AND ANALYSIS OF CLUSTERS AND NANOPARTICLES

by

PHILLIP BENSON HAM III

(Under the Direction of Michael A. Duncan)

ABSTRACT

Laser desorption mass spectrometry was used in the production and analysis of gas phase metal sulfur clusters. Clusters of gas phase aluminum, gallium, and indium sulfur were produced and analyzed using a time-of-flight mass spectrometer. Also, carbon nano-onions produced by an arc between graphite electrodes in water and the annealing of nanodiamonds were analyzed. The sulfur experiments were done by mixing metal powders with sulfur and vaporizing the mixture with a laser. The mass spectra reveal that certain gas phase clusters are stable when they satisfy electron counting rules. This gas phase correspondence in stability to condensed phase studies suggests that well-developed structure and bonding ideas can be applicable for understanding the stability and structure of gas phase clusters. Furthermore, we measured the first known mass spectrum of carbon nano-onions. Production methods and "peeling" reactions with these species are compared based on the mass of the nano-onions.

INDEX WORDS: Laser vaporization, Laser desorption, Gas phase synthesis, Nanoparticles, Metal sulfur clusters, Carbon onions

PRODUCTION AND ANALYSIS OF CLUSTERS AND NANOPARTICLES

by

PHILLIP BENSON HAM III

B.S. The University of Georgia, 2007

A Thesis Submitted to the Graduate Faculty of The University of Georgia in Partial Fulfillment of the Requirements for the Degree

MASTER OF SCIENCE

ATHENS, GEORGIA

2007

PRODUCTION AND ANALYSIS OF CLUSTERS AND NANOPARTICLES

by

PHILLIP BENSON HAM III

Major Professor: Michael A. Duncan

Committee: Nigel Adams
Jonathan Amster

Electronic Version Approved:

Maureen Grasso
Dean of the Graduate School
The University of Georgia
May 2007

ACKNOWLEDGMENTS

First of all, I would like to thank God for sending His Son for us. Without that, life would have no hope. I also thank God for giving me the strength to finish this thesis. Many times the verses from Isaiah 40:28-31 have given me hope and new strength.

"Do you not know? Have you not heard?
The Everlasting God, the LORD, the Creator of the ends of the earth
Does not become weary or tired
His understanding is inscrutable.
He gives strength to the weary,
And to him who lacks might He increases power.
Though youths grow weary and tired,
And vigorous young men stumble badly,
Those who wait for the LORD
Will gain new strength;
They will mount up with wings like eagles,
They will run and not get tired,
They will walk and not become weary."
-Isaiah 40:28-31

Thank you God for giving strength to me when I have been weary or stumbled. I would also like to thank my wife for being such a great helper. God has truly blessed me through you, and I thank Him for giving me such a good and perfect gift (James 1:17). I would like to thank my family for their discipline, guidance, support, and encouragement over the years. When you "train a child in the way he should go... when he is old he will not turn from it." (Proverbs 22:6) Through I may not have expressed appreciation at the time, I am grateful for your training. Finally, I would like to thank Dr. Duncan and my research group. Your patience, counsel, and help have been vital. Dr. Duncan, I thank you for helping me as we traveled new ground together through the BS/MS program. A fourth year college student finishing a Masters thesis requires a special professor. I have an incredible amount of respect for you.

TABLE OF CONTENTS

Page

CHAPTER 1

INTRODUCTION AND LITERATURE REVIEW

1.1 HISTORY

An ancient question in chemistry has been, "How much can you divide a substance and its properties remain the same?" The famous scientist James Clerk-Maxwell believed this ancient question was answered when he published his paper on water molecules.[1] For example, if you take a drop of water and divide it in half, the result is two portions of the same substance that are the equivalent to the original substance except for their size. Continue this division process until you can go no further and the final result is an atom or molecule. According to Maxwell, molecules are the smallest indivisible particles that retain the properties of the bulk.[1] However, the fields of nanoscience and clusters have challenged these long held theories. Generally, clusters are aggregations of less than 100 atoms while nanoparticles are aggregations of atoms about a nanometer in size. Typically, aggregations of more than 100 atoms are referred to as nanoparticles. These clusters and nanoparticles are extremely interesting for study because their size contributes to distinctive chemical, physical, optical, and magnetic properties.[5-9] Elements gain totally different properties at small sizes because their bonding must fundamentally change to satisfy unfilled valence shells. In fact, cluster and nanoscience research is finding many cases where the properties of just a few atoms are radically different from the properties of moles of atoms. A peculiar part of nanoscience is that man has unknowingly been using small nano-sized materials for hundreds of years.

There are many examples of clusters used before their sizes were known. The cluster calomel, Hg_2Cl_2, was known in India in the 12^{th} century and was used medicinally as a disinfectant. Solutions of gold colloid particles less than 100 nm in size were used to produce the bright red in the stained-glass windows of cathedrals as shown in Figure 1.1. In 1857, the famous scientist Michael Faraday surmised that the bright red color of colloidal gold was due to

the extremely small size of the gold particles, although he lacked the experimental means necessary to confirm his hypothesis.[2] Furthermore, brightly colored nanometer-sized colloidal particles were used in cave paintings made by ancient humans thousands of years ago in Lascaux, France. These small particles were made by hydrophobically stabilizing mixtures of minerals to create brightly colored particles with diameters of 100 nm or less.[3] Thus, the properties of nanoparticles were used long before the actual science existed.

1.2 BIOLOGICAL METAL SULFUR CLUSTERS

Particles that are smaller than nanoparticles and consist of fewer than 100 atoms are called clusters. Clusters are extremely important in biology because the active sites of many enzymes are composed of metal sulfur clusters. For example, iron-sulfur clusters are present at the active site of electron transport proteins such as ferredoxin.[4-7] They function as capacitors that receive, store, and disburse charge in the mitochondrial membrane. Thus, although they are tiny compared to the protein, iron-sulfur proteins affect the function of the entire protein due to their unique properties. Another critical enzyme with metal sulfur clusters in biology is nitrogenase. Nitrogenases are a family of enzymes that have molybdenum-iron-sulfur clusters at their active site and are crucial for nitrogen fixation; nitrogenase uses molybdenum-iron-sulfur clusters to break the extremely strong triple bond of N_2 and form ammonia.[8-11] Without these clusters, the enzyme would not function, and nitrogen needed for amino acid and protein production would be unavailable. NADH dehydrogenase also has iron-sulfur clusters. It has eight iron-sulfur clusters among its 45 separate polypeptide chains. It catalyzes the oxidation of NADH and reduction of coenzyme Q in the electron transport chain for ATP synthesis. Thus, metal-sulfur clusters are extremely important in biology for their role in mitochondrial electron

transport, ATP formation, and nitrogen fixation, as well as photosynthetic electron transport, pyruvate metabolism, and hydrogen uptake.[12, 13]

1.3 INORGANIC CLUSTERS AND NANOSCIENCE

Advances in clusters and nanoscience have revolutionized the field of inorganic chemistry. A brave new "small" world now characterizes many fields of inorganic materials research. Scientists are looking at old materials in new ways where "size matters." In several cases, scientists considered many of these materials to have little chemical reactivity or relevance. Groundbreaking research in areas such as the study of gold nanoparticles, semiconductor quantum dots, and fullerene chemistry is transforming the field of science, providing new materials, and showing that nanoscience has broad and profound implications.

Metal clusters exhibit trends in their stoichiometries and bonding. The clusters of alkali and alkaline earth metals often form Jellium clusters, where their extra electrons form "superatom" valence shells. Clusters of transition metals generally exist in statistical distributions, while main group metals may exist as Wade's rules clusters, clusters that have increased stability from 3D aromaticity. These bonding models have been used to explain the size distributions of many cluster systems.

1.3.1 GOLD NANOPARTICLES

Gold is unreactive in the bulk. It forms few compounds, is not easily ionized, and has been considered the most noble of all metals.[14, 15] As a result of its unreactivity, attractive yellow color, rarity, and luster, it is often used in jewelry. However, at small sizes, its reactivity,[16-24] color, [2, 25] and other optical properties[26-28] completely change.

Methods for the production of gold nanoparticles are varied and diverse. Colloidal gold nanoparticles can be prepared by reduction of chloroauric acid with

tetrakis(hydroxymethyl)phosphonium chloride in an alkaline solution.[29] Over a four month time period that the particles were in solution, they were observed to grow larger as time passed.[29] Other methods of gold nanoparticle production are coprecipitation or deposition precipitation of $Au(OH)_3$, grafting of organo-gold complexes such as dimethyl-Au(III)-acetylacetonate, mixing of colloidal Au particles, and vacuum deposition.[16] For many applications, these nanoparticles must be deposited on support materials. Metal oxide and carbon surfaces are commonly used for this purpose, and the support material may change the nanoparticles properties.[16]

The "most noble of all metals"[15] actually becomes an extremely reactive catalyst in particles consisting of less than 10-20 atoms.[19] When deposited on metal oxide surfaces, gold is active in catalysis of the combustion of CO and saturated hydrocarbons[30]; the oxidation-decomposition of amines and organic halogenated compounds[31]; the partial oxidation of hydrocarbons[30]; the hydrogenation of carbonyl compounds, alkynes and alkadienes[32]; and the reduction of nitrogen oxides.[23]

The color of gold colloid nanoparticles is size-dependent. They can be bright red or purple based on their dimensions.[2, 25] These bright colors are caused by surface plasmon resonances (SPR).[33] SPR occurs when a fraction of the light energy incident upon a surface interacts with the delocalized electrons in the metal and, as a result, resonant colors of light are absorbed. The structure and size of the gold particle affect the delocalized electron resonances; thus, by manipulating the size of the colloidal gold particles, the color of the particles can be altered.

Moreover, gold nanoparticles are currently being investigated as a cancer treatment. Their derivatives exhibit size-dependent selectivity for binding to cancer cell biomarkers. Selectivity is a requirement because the treatment must focus on killing the cancer cells, not the

entire body. Then, because of the unique optical properties of gold nanoparticles, they could be exploited in cancer photodiagnostics and photothermal therapy.[26-28] The cancer cells can be found based on where the gold is concentrated in the body. Since the body is transparent to certain wavelengths of infrared light and gold nanoparticles in cancer cells would absorb this wavelength, the cancer can be treated by shining a laser on the tumor.

Other unreactive jewelry metals like platinum, palladium, and silver can also be produced as nanoparticles and studied in similar ways.[34] Like gold nanoparticles, they are being studied for their catalytic value.[34] Since they are so new, many other potential applications have not yet been discovered. Hence, even "unreactive," "uninteresting" elements can be chemically, physically, and medicinally significant on the nanoscale.

1.3.2 QUANTUM DOTS

The study of quantum dots is another exciting area in the fields of inorganic chemistry and nanotechnology. Quantum dots typically consist of semiconductor elements, are on the order of a nanometer in size, and have distinctive size-dependent optical properties.[35] Because these particles are so small, the electrons within them are confined to a volume that is about the size of the particle, which is also about the size of the deBroglie wavelength of an electron. Therefore, quantum dots can be modeled by a particle-in-a-box approach that generates discrete energy levels that are spaced based on the size of the box.[35] While the elements that constitute the quantum dots play a role in the spacing of the energy levels, size is the primary factor. The energy levels of small quantum dots are farther apart than the energy levels of large quantum dots. Electronic transitions between energy levels cause fluorescence at specific wavelengths based on their spacing. Consequently, small quantum dots emit bluer light while large quantum dots emit redder light.[35]

A number of the first examples of semiconductor quantum dots were produced in the 1980s. Gallium arsenide and aluminum gallium arsenide were produced by Reed and coworkers.[36] Then, Brus and coworkers found that the absorbance of CdSe quantum dots could be manipulated by changing their size.[37,38] Now, many production techniques exist including electron beam lithography,[39, 40] reactive ion etching,[41-43] pyrolytic processes,[44, 45] colloidal suspensions,[37, 46, 47] and heating followed by crystallization.[48-50] Colloidal synthesis is considered the cheapest, easiest (benchtop method), and least toxic wet chemistry method of preparing quantum dots. In this process, precipitation reactions yield dilute suspensions of *quasi* monodispersed particles. Monodisperse particles, particles that are the same size, are desired because properties are size-dependent. Precipitation is often catalyzed by seeds of very small particles for the subsequent growth of larger ones. Colloidal nanoparticle synthesis by precipitation begins with adding together two separate dilute aqueous solutions containing salts of the desired quantum dot elements. Precipitation starts on the seed crystals and the dots continue growing. Since the precipitation is an equilibrium process in a dilute solution, crystallized particles may redissolve. Because of their greater surface area, smaller particles are much more likely to redissolve in the dynamic equilibrium. The redissolved particles may then add onto the larger particles, causing them to grow further (Ostwald ripening).[51] Larger particles are grown by allowing the reaction to occur for a greater amount of time. Once the desired time/size is reached, organic surfactants are added as a capping agent to prevent further growth or reactions. This method can be used to produce nanocrystalline materials.[52] If smaller particles are desired, then organic solvents such as acetonitrile or hexane may be used or organic substances such as styrene/maleic anhydride copolymer may be added to the aqueous solution. This method produces particles between 34 and 43 Å, respectively.[40] Cubic ZnS and CdS

nanocrystallites were synthesized in aqueous and methanol solutions. In this manner, specific-sized quantum dot nanoparticles can be synthesized.[39]

Since quantum dots have an enormous variety of properties, they are currently being considered for numerous applications. Because of their optical properties, quantum dots may be used in diode lasers, biological sensors, photovoltaic cells,[53] and light-emitting diodes.[54, 55] Furthermore, their electronic properties make them useful as semiconductors. Linked quantum dots may provide a means for quantum computing where calculations are performed at many times the current rate.[56] The applications of quantum dots may vary as much as their size range as new mass production and refining methods are made available.

1.3.3 FULLERENES, CARBON NANOTUBES, AND CARBON ONIONS

The study of fullerenes is an important area in nanoparticle research. The production and observation of C_{60} in a molecular beam mass spectrometer by Curl, Kroto, and Smalley was a serendipitous discovery.[57] They had been planning to investigate long-chain hydrocarbons in red giant stars by mimicking their environment in a laser plasma, but instead they found a new allotrope of carbon, which they named buckminsterfullerene.[58] They suggested that it had a spherical shape, truncated icosahedral symmetry, and carbon atoms arranged in pentagons and hexagons much like a soccer ball.[59] Each molecule has 32 interlocking rings (20 hexagons and 12 pentagons). Its atomic geometry suggested a three-dimensional network of sp^2 hybridized atoms where each carbon is attached to three nearest neighbors through σ orbitals. The remaining p orbital would form a partially shared π bond with its neighbors.[60] However, despite the rationale for its existence, C_{60} remained a curiosity until it was produced in the condensed phase.[59]

In 1990, Kratschmer and Huffman produced C_{60} in the condensed phase. They used an arc between graphite electrodes in 13 kPa helium.[61] They found that C_{60} is 10% of the soot product and that it is soluble in benzene, dicloromethane, chloroform, and many other organic solvents.[59, 60, 62] Then, they verified the anticipated structure using IR spectroscopy and X-ray diffraction.[61] In the IR spectrum, only four lines were observed- those at 1429, 1183, 577, and 528 cm^{-1}. This confirmed the icosahedral structure.[63] It was also purified using chromatography in an alumina column with hexane as the solvent.[62] Thus, C_{60} became readily available for widespread investigation.

As a result of C_{60}'s availability, many new properties and potential applications were discovered. Because fullerenes are essentially hollow cages, they can be adapted to make materials never before known. For example, metal atoms can fit inside the cage and form endohedral structures.[60] In fact, endohedral potassium atoms of the form M_3C_{60} exhibit high temperature superconductivity, and this property was found to apply to cesium, rubidium, sodium, and lithium endohedral structures as well.[64, 65] Additionally, in the structure of C_{60}, the five membered rings avoid double bond character because this reduces strain and prevents the molecule from being antiaromatic. Therefore, these sites lack electron density and are electrophilic. When a nucleophile is present, nucleophilic additions usually occur at the pentagonal carbons.[60] Thus, C_{60} can be functionalized for use in polymers, catalysis, and drug delivery systems.[59] C_{60} is even being considered for the treatment of AIDS. An important enzyme for AIDS virus replication has a nonpolar pocket where functionalized C_{60} can bind. In this way, a C_{60} derivative could inhibit the AIDS virus.[66] The discovery of C_{60} is another important example of how basic research on small nanomaterials can be extremely valuable.

C_{60}'s discovery led to the search for other new allotropes. Carbon nanotubes were the next structure to be found.[59, 67] They are essentially C_{60} expanded like graphite in one dimension. They can be produced via an arc discharge in liquid nitrogen,[68] in the gas phase (1 nm diameter single walled carbon nanotubes),[69] by condensation of a laser-vaporized carbon-nickel-cobalt mixture,[70] and by the catalytic chemical vapor deposition of methane.[71] Nanotubes have the largest known Young's modulus and tensile strength, so they could be used as super-strong construction materials.[59] Also, they have tunable mechanical, electrical, and magnetic properties based on their diameter.[59, 69, 72, 73] Researchers are particularly excited about the electrical properties of nanowires because they could be used to build nanocircuits for electronic devices.[73] Crossed nanowires have even demonstrated logic functions![73-75] Computers in the future could have nanowire structures to perform calculations. These awesome properties have led to very enthusiastic scientific research.

Later, carbon nano-onions, the fifth allotrope of carbon, were discovered.[76] Carbon onions consist of spheres of carbon nested inside each other like Russian dolls. Generally, carbon onions have C_{60} molecules at their core, and larger spheres such as C_{240} and C_{540} compose the outer layers. Carbon onions form because small graphene sheets have dangling bonds on their edges, so the sheets bend in a circle to bond their unbound edges together. When several adjacent sheets do this, large multi-shelled fullerenes form. Carbon onions can be produced by electron beam irradiation of amorphous carbon in a transmission electron microscope,[76-78] by the annealing of nanodiamonds at 1500-1700ºC,[79] implantation of 120 keV carbon ions into silver resulting in the precipitation of carbon onions,[80] by radio-frequency plasma-enhanced chemical vapor deposition,[81] and by using an arc between graphitic electrodes in water.[82] In the arc method of production, Sano and coworkers observed that carbon onions float! This was

surprising because the density of carbon onions is greater than water. They suggested that this occurs because of the carbon onions' hydrophobicity.[82] However, Rettenbacher and coworkers found that carbon onions were also present in the bottom of the water container.[83] Currently, the two primary carbon onion production methods are 1) the annealing of nanodiamonds and 2) an arc discharge in water. These methods supposedly produce different size carbon onions with different properties.[84] While much work has been done on C_{60}, carbon nanotubes, and carbon onions, no mass spectrometry measurements have been made. The only size verification experiments that have been done so far are electron microscopy. These cannot accurately verify their sizes or their distribution.

1.3.4 THE POLYHEDRAL SKELETAL ELECTRON PAIR THEORY

The polyhedral skeletal electron pair theory, also known as "Wade's rules," predicts structure and stability for certain kinds of electron deficient clusters.[13] They were first found to apply to borane,[85, 86] carborane,[87] and metal carbonyl clusters.[88] $B_6H_6^{2-}$ was the first system discovered, and other $B_nH_n^{2-}$ species followed soon after.[13, 86] The carborane species are similar in that an isoelectronic CH group replaces a BH^- group.[13] Thus, carboranes of this form typically exist as neutral $B_{n-2}C_2H_n$. These systems have been prepared from n=6 to 10.[13] These systems are called closo because shared electron density is "closed" inside a polyhedron whose vertices are atoms. Since not enough electrons are available for bonding in these clusters, they share p electrons at the center of the structure in a type of 3D aromaticity.[13] Clusters having these structures were found to be more stable than most other clusters with slight variations. However, some clusters with slight variations were found to be stable as well. These came to be known as nido and arachno species. $B_7C_2H_{13}$ is an example of a nidocarborane. Nido clusters have an open face and arachno clusters have two open faces. Arachnoborane species are more rare, although other metal clusters have this

geometry.[13] Electron counting showed that these clusters are stable when they have a numerical relationship between the number of atoms on the vertices of a polyhedron, N, and the number of skeletal electrons. Closo clusters have 2N+2 electrons, nido clusters have 2N+4 electrons, and arachno clusters have 2N+6 electrons.[13, 89-91] Metal clusters have also been found to follow these rules. Some of the first examples of these are now known as "Zintl" ions after their discoverer. He observed that clusters of Sn_5^{2-}, Pb_5^{2-}, Pb_9^{4-}, Bi_9^{5+}, and Ge_9^{4-} form when these metals are dissolved in liquid ammonia.[92] While these clusters were known to be stable, it was initially not known why. It was discovered much later that these clusters satisfied Wade's rules.[93, 94]

1.3.5 THE JELLIUM MODEL

While electron poor species may form Wade's rules clusters, electron rich species may form spherical Jellium clusters. Jellium species were first observed by Knight and coworkers in mass spectrometry experiments of sodium clusters.[95] They observed magic numbers at 8, 20, 40, 58, and 92 atoms of sodium. They attributed this nonstatistical distribution to "a one-electron shell model in which independent delocalized atomic 3*s* electrons are bound in a spherically symmetric potential well.[95]" In other words, they suggested that the sodium nuclei and closed shells collapse together in a sort of superatom, while the extra 3s electrons are located in superatom orbitals similar to the orbitals in atoms. Since experiments with other elements with different numbers of electrons confirmed these distributions, observed valence shell closings at 8, 20, 40, 58, etc., electrons were suggested.[95-98] These made sense in terms of the orbitals listed in Table 1.1. Like normal atoms, superatoms are most stable when they have a closed shell of electrons in this new counting scheme. Therefore, superatoms with more electrons than a full shell lose that electron very easily, like an alkali or alkaline metal, while superatoms with more than a full shell of electrons should have a large electron affinity, like a halogen.[97, 98]

1.3.6 GAS PHASE CLUSTERS

A prerequisite for many types of industrial applications is stability. Metal carbide, oxide, and sulfide systems have high bond energies and high stability relative to metal atom clusters. Thus, these systems are expected to be more relevant for applications than metal atom clusters. Furthermore, their higher bond energies make them much more likely to be isolated in the condensed phase. However, condensed phase cluster and nanoparticle studies often require unique step-by-step production methods. Because of this, gas phase metal compound clusters of these elements have been investigated intensely.

Gas phase production methods offer several advantages over wet chemistry methods. For many electronic applications, impurities in semiconductors can be catastrophic. Solution phase methods commonly introduce impurities while gas phase methods do not. Gas phase methods have another advantage in that they are continuous and can produce more uniform products than solution methods. Gas phase production procedures do not have the "batch problem" of condensed phase methods. In general, solution phase methods are quantitatively better, while gas phase methods are qualitatively better.[99] Therefore, as was the case with C_{60}, gas phase methods of production and study may be done before the particle has been isolated in the condensed phase. While many nanoparticles and clusters are being studied in the gas phase, metal main-group compounds such as metal carbides, oxides, and sulfides are some of the systems that are of particular interest to our group.

In 1992, Castleman and coworkers introduced a “new class of molecular clusters” by reporting the magic number in titanium carbide clusters at $Ti_8C_{12}^+$.[100] These clusters were named metallocarbohedrenes, or “met-cars” for short, and proposals concerning their structure commenced shortly after their discovery. Met-car clusters with other metals (V, Zr, Hf) also followed,[101] and a

cage structure with dodecahedral symmetry was suggested, although it is not yet confirmed.[102] Soon after, another magic number at $Ti_{14}C_{13}^{+}$ was reported and magic numbers of this stoichiometry with other metals (Cr, Mo, Fe) were also found.[103-105] When magic numbers such as $Ti_{14}C_{13}^{+}$ and $Ti_8C_{12}^{+}$ exist in mass spectra, they can be the result of special stability caused by structural, electronic, or other factors. In fact, the stability of the $Ti_{14}C_{13}^{+}$ cluster is believed to be due to its structure; it has a face centered cubic lattice with a 3x3x3 (27 atoms) arrangement comparable to NaCl.[103] Also, the $Ti_{14}C_{13}$ cluster is one atom different from the NaCl stoichiometry. Thus, it can be considered a cubic fragment of the larger lattice. Larger structures were also found (e.g. 4x4x4, 5x5x5, etc) and thus, these clusters are known as nanocrystals. IR spectroscopy was performed on these clusters using a free electron laser for infrared experiments,[103, 106] and infrared resonance enhanced multiphoton ionization (IR-REMPI) measurements confirmed their structure. Incidentally, the nanocrystal spectra matched beautifully with both a solid-state rock salt TiC surface and with infrared emissions from post asymptotic giant branch (AGB) stars.[106, 107] Thus, in an unlikely combination of experiments, titanium carbide nanocrystals were found to be components of star dust. Because they are found in the center of meteorites, they appear to be one of the first things to coalesce in the hot plasma environment of aging post AGB stars.[107] Therefore, these clusters have astronomical importance in addition to their catalytic properties.[108]

Metal oxide clusters are another type of metal compound cluster that may have unique properties and that can be easily studied in the gas phase. Metal oxide clusters are known for applications in catalysis, electronics, and ceramics.[109-112] Many studies of metal oxides have been done,[113-121]and gas phase metal oxide clusters do not exhibit a statistical distribution; rather, they exhibit only a limited number of stoichiometries. The number of oxygen atoms is typically greater than the number of metal atoms in these experiments.[122] Photodissociation experiments on these

clusters suggest that these clusters exist as a stable, strongly bonded core with extra oxides on the surface; oxygen atoms are eliminated until the stable core is reached. Also, mass spectra of many metal oxides have been studied, including Zr, Ti, Mg, Al, In, and Ga oxides.[118, 119, 123, 124] In the mass spectra, Al, In, and Ga oxide clusters are observed in nonstatistical distributions of the form $MO^+(M_2O_3)_n$.[125-129] These studies observed that the prevalence of certain ions in the metal oxide mass spectra was not merely a statistical fluctuation; the structure and electronic arrangement of the ions determine their stability.

Gas phase cluster studies can offer significant advantages over condensed phase studies because of their ability to differentiate between very similar particles, to synthesize these particles in a pure environment, and to analyze them quickly. In fact, the met-car species have not yet been isolated in the condensed phase, yet much experimental data has already been collected for this species. While condensed phase production methods are good because they produce nanoparticles for study in large quantities, gas phase measurements are efficient and effective means of investigating many nanoparticles.

1.4 REFERENCES

1. Clerk-Maxwell, J., Molecules. *Nature* **1873,** 8, 437-441.

2. Faraday, M., *Philosophical Transactions* **1857,** 147, 145.

3. Brinker, C. J.; Scherer, G. W., *Sol-Gel Science: The Physics and Chemistry of Sol-Gel Processing*. Academic Press: London, 1990.

4. Bruschi, M.; Guerlesquin, F., Structure, Function and Evolution of Bacterial Ferredoxins. *FEMS Microbiol. Rev.* **1988,** 54, (2), 155-175.

5. Brettel, K.; Leibl, W., Electron transfer in photosystem I. *Biochimica Et Biophysica Acta-Bioenergetics* **2001,** 1507, (1-3), 100-114.

6. Setif, P., Ferredoxin and flavodoxin reduction by photosystem I. *Biochimica Et Biophysica Acta-Bioenergetics* **2001,** 1507, (1-3), 161-179.

7. Vassiliev, I. R.; Antonkine, M. L.; Golbeck, J. H., Iron-sulfur clusters in type I reaction centers. *Biochimica Et Biophysica Acta-Bioenergetics* **2001,** 1507, (1-3), 139-160.

8. Coucouvanis, D., Recent Structure Determinations of the Molybdenum Iron Protein of Nitrogenase - Impact on Design of Synthetic Analogs for the Iron Molybdenum Sulfur Active-Site and the Iron Molybdenum Cofactor. *ACS Symposium Series* **1993,** 535, 304-331.

9. Dance, I., Theoretical investigations of the mechanism of biological nitrogen fixation at the FeMo cluster site. *J. Biol. Inorg. Chem.* **1996,** 1, (6), 581-586.

10. Coucouvanis, D., Functional analogs for the reduction of certain nitrogenase substrates. Are multiple sites within the Fe/Mo/S active center involved in the 6e(-) reduction of N-2? *J. Biol. Inorg. Chem.* **1996,** 1, (6), 594-600.

11. Seefeldt, L. C.; Dance, I. G.; Dean, D. R., Substrate interactions with nitrogenase: Fe versus Mo. *Biochemistry* **2004,** 43, (6), 1401-1409.

12. Mingos, D. M. P.; Wales, D. J., *Introduction to Cluster Chemistry*. Prentice Hall: Englewood Cliffs, 1990

13. Cotton, F. A.; Wilkinson, G.; Murillo, C.; Bochmann, M., *Advanced Inorganic Chemistry, 6th ed.* John Wiley & Sons, Inc.: New York, 1999.

14. Brown, T. L.; LeMay, H. E.; Bursten, B. E.; Burdge, J. R., *Chemistry: The Central Science*. 9th ed.; Pearson Education, Inc.: Upper Saddle River, 2003.

15. Hammer, B.; Norskov, J. K., Why Gold Is the Noblest of All the Metals. *Nature* **1995,** 376, (6537), 238-240.

16. Haruta, M., Gold as a novel catalyst in the 21st century: Preparation, working mechanism and applications. *Gold Bull.* **2004,** 37, (1-2), 27-36.

17. Haruta, M., Nanoparticulate gold catalysts for low-temperature CO oxidation. *J. New Mat. Electr. Sys.* **2004,** 7, (3), 163-172.

18. Sinha, A. K.; Seelan, S.; Tsubota, S.; Haruta, M., Catalysis by gold nanoparticles: epoxidation of propene. *Top. Catal.* **2004,** 29, (3-4), 95-102.

19. Haruta, A., When gold is not noble: Catalysis by nanoparticles. *Chem. Rec.* **2003,** 3, (2), 75-87.

20. Haruta, M., Catalysis of gold nanoparticles deposited on metal oxides. *Cattech* **2002,** 6, (3), 102-115.

21. Akita, T.; Tanaka, K.; Okuma, K.; Koyanagi, T.; Haruta, M., TEM and HAADF-STEM study of a Au catalyst supported on a TiO2 nano-rod. *J. Electron Microsc.* **2001,** 50, (6), 473-477.

22. Haruta, M.; Souma, Y., Copper, silver and gold in catalysis - Preface. *Catal. Today* **1997,** 36, (1), 1-1.

23. Haruta, M., Size- and support-dependency in the catalysis of gold. *Catal. Today* **1997,** 36, (1), 153-166.

24. Haruta, M., Surface chemistry in heterogeneous catalysis. *Journal of Japanese Society of Tribologists* **1997,** 42, (9), 706-711.

25. Kelly, K. L.; Coronado, E.; Zhao, L. L.; Schatz, G. C., The optical properties of metal nanoparticles: The influence of size, shape, and dielectric environment. *J. Phys. Chem. B* **2003,** 107, (3), 668-677.

26. El-Sayed, I. H.; Huang, X. H.; El-Sayed, M. A., Selective laser photo-thermal therapy of epithelial carcinoma using anti-EGFR antibody conjugated gold nanoparticles. *Cancer Letters* **2006,** 239, (1), 129-135.

27. Huang, X. H.; El-Sayed, I. H.; Qian, W.; El-Sayed, M. A., Cancer cell imaging and photothermal therapy in the near-infrared region by using gold nanorods. *J. Am. Chem. Soc.* **2006,** 128, (6), 2115-2120.

28. Jain, P. K.; El-Sayed, I. H.; El-Sayed, M. A., Au nanoparticles target cancer. *Nano Today* **2007,** 2, (1), 18-29.

29. Grunwaldt, J. D.; Kiener, C.; Wogerbauer, C.; Baiker, A., Preparation of supported gold catalysts for low-temperature CO oxidation via "size-controlled" gold colloids. *J. of Catal.* **1999,** 181, (2), 223-232.

30. Arenz, M.; Landman, U.; Heiz, U., CO combustion on supported gold clusters. *ChemPhysChem* **2006,** 7, (9), 1871-1879.

31. Arcadi, A.; Di Giuseppe, S., Recent applications of gold catalysis in organic synthesis. *Curr. Org. Chem* **2004,** 8, (9), 795-812.

32. Sakurai, H.; Tsubota, S.; Haruta, M., Hydrogenation of CO_2 over Gold Supported on Metal-Oxides. *Applied Catalysis a-General* **1993,** 102, (2), 125-136.

33. Mazzoldi, P.; Arnold, G. W.; Battaglin, G.; Gonella, F.; Haglund, R. F., Metal nanocluster formation by ion implantation in silicate glasses: Nonlinear optical applications. *Journal of Nonlinear Optical Physics & Materials* **1996,** 5, (2), 285-330.

34. Welch, C. W.; Compton, R. G., The use of nanoparticles in electroanalysis: a review. *Anal. Bioanal. Chem.* **2006,** 384, (3), 601-619.

35. Jacak, L.; Hawrylak, P.; Wójs, A., *Quantum Dots*. Springer: Berlin, 1998; p 176.

36. Reed, M. A.; Bate, R. T.; Bradshaw, K.; Duncan, W. M.; Frensley, W. R.; Lee, J. W.; Shih, H. D., Spatial quantization in gallium arsenide-aluminum gallium arsenide multiple quantum dots. *Journal of Vacuum Science & Technology, B: Microelectronics and Nanometer Structures* **1986,** 4, (1), 358-360.

37. Brus, L., Electronic Wave-Functions in Semiconductor Clusters - Experiment and Theory. *J. Phys. Chem.* **1986,** 90, (12), 2555-2560.

38. Steigerwald, M. L.; Alivisatos, A. P.; Gibson, J. M.; Harris, T. D.; Kortan, R.; Muller, A. J.; Thayer, A. M.; Duncan, T. M.; Douglass, D. C.; Brus, L. E., Surface Derivatization and Isolation of Semiconductor Cluster Molecules. *J. Am. Chem. Soc.* **1988,** 110, (10), 3046-3050.

39. Randall, J. N.; Reed, M. A.; Kao, Y. C., Fabrication of Closely Spaced Quantum Dot Diodes. *Journal of Vacuum Science & Technology B* **1990,** 8, (6), 1348-1352.

40. Marzin, J. Y.; Izrael, A.; Birotheau, L., Optical-Properties of Etched GaAs/GaAlAs Quantum Wires and Dots. *Solid-State Electron.* **1994,** 37, (4-6), 1091-1096.

41. Watt, M.; Sotomayortorres, C. M.; Cheung, R.; Wilkinson, C. D. W.; Arnot, H. E. G.; Beaumont, S. P., Raman-Scattering Investigations of the Damage Caused by Reactive-Ion-Etching of GaAs. *Superlattices Microstruct.* **1988,** 4, (2), 243-244.

42. Watt, M.; Sotomayortorres, C. M.; Cheung, R.; Wilkinson, C. D. W.; Arnot, H. E. G.; Beaumont, S. P., Raman-Scattering of Reactive-Ion Etched GaAs. *J. Mod. Opt.* **1988,** 35, (3), 365-370.

43. Forchel, A.; Maile, B. E.; Leir, H.; Germann, R., *Physics and Technologies of Submicron Structures*. Springer: Berlin, 1988; Vol. 83, p 26.

44. Medeiros-Ribeiro, G.; Ohlberg, D. A. A.; Williams, R. S.; Heath, J. R., Rehybridization of electronic structure in compressed two-dimensional quantum dot superlattices. *Phys. Rev. B* **1999,** 59, (3), 1633-1636.

45. Mu, R.; Tung, Y. S.; Ueda, A.; Henderson, D. O., Chemical and size characterization of layered lead iodide quantum dots via optical spectroscopy and atomic force microscopy. *J. Phys. Chem.* **1996,** 100, (51), 19927-19932.

46. Littau, K. A.; Szajowski, P. J.; Muller, A. J.; Kortan, A. R.; Brus, L. E., A Luminescent Silicon Nanocrystal Colloid Via a High-Temperature Aerosol Reaction. *J. Phys. Chem.* **1993,** 97, (6), 1224-1230.

47. Michaels, A. M.; Nirmal, M.; Brus, L. E., Surface enhanced Raman spectroscopy of individual rhodamine 6G molecules on large Ag nanocrystals. *J. Am. Chem. Soc.* **1999,** 121, (43), 9932-9939.

48. Ekimov, A. I.; Efros, A. L.; Onushchenko, A. A., Quantum Size Effect in Semiconductor Microcrystals. *Solid State Commun.* **1985,** 56, (11), 921-924.

49. Ekimov, A. I.; Onushchenko, A. A., Quantum Size Effect in 3-Dimensional Microscopic Semiconductor Crystals. *JETP Letters* **1981,** 34, (6), 345-349.

50. Ekimov, A. I.; Onushchenko, A. A., Quantum Size Effect in the Optical-Spectra of Semiconductor Micro-Crystals. *Soviet Physics Semiconductors-USSR* **1982,** 16, (7), 775-778.

51. Rossetti, R.; Ellison, J. L.; Gibson, J. M.; Brus, L. E., Size Effects in the Excited Electronic States of Small Colloidal CdS Crystallites. *J. Chem. Phys.* **1984,** 80, (9), 4464-4469.

52. Trindade, T.; O'Brien, P.; Pickett, N. L., Nanocrystalline semiconductors: Synthesis, properties, and perspectives. *Chem. Mater.* **2001,** 13, (11), 3843-3858.

53. Reed, M. A., Quantum Dots. *Scientific American* 1993, p 118.

54. Coe, S.; Woo, W. K.; Bawendi, M.; Bulovic, V., Electroluminescence from single monolayers of nanocrystals in molecular organic devices. *Nature* **2002,** 420, (6917), 800-803.

55. Stevenson, R. M.; Young, R. J.; Atkinson, P.; Cooper, K.; Ritchie, D. A.; Shields, A. J., A semiconductor source of triggered entangled photon pairs. *Nature* **2006,** 439, (7073), 179-182.

56. Kastner, M. A., Prospects for quantum dot implementation of adiabatic quantum computers for intractable problems. *Proceedings of the IEEE* **2005,** 93, (10), 1765-1771.

57. Kroto, H. W.; Heath, J. R.; Obrien, S. C.; Curl, R. F.; Smalley, R. E., C-60 - Buckminsterfullerene. *Nature* **1985,** 318, (6042), 162-163.

58. Kroto, H., Space, Stars, C-60, and Soot. *Science* **1988,** 242, (4882), 1139-1145.

59. Dresselhaus, M. S.; Dresselhaus, G.; Eklund, P., *Science of Fullerenes and Carbon Nanotubes*. Academic Press, Inc.: San Diego, 1996; p 965.

60. Billups, W. E.; Ciuolini, M. A., *Buckminsterfullerenes*. VCH Publishers, Inc.: New York, 1993.

61. Kratschmer, W.; Lamb, L. D.; Fostiropoulos, K.; Huffman, D. R., Solid C-60 - a New Form of Carbon. *Nature* **1990,** 347, (6291), 354-358.

62. Taylor, R.; Hare, J. P.; Abdulsada, A. K.; Kroto, H. W., Isolation, Separation and Characterization of the Fullerenes C-60 and C-70 - the 3rd Form of Carbon. *Journal of the Chemical Society-Chemical Communications* **1990**, (20), 1423-1424.

63. Gadalla, A., Solid C-60 - Preparation and Characterization. *International Journal of Electronics* **1994,** 77, (2), 193-198.

64. Haddon, R. C.; Hebard, A. F.; Rosseinsky, M. J.; Murphy, D. W.; Duclos, S. J.; Lyons, K. B.; Miller, B.; Rosamilia, J. M.; Fleming, R. M.; Kortan, A. R.; Glarum, S. H.; Makhija, A. V.; Muller, A. J.; Eick, R. H.; Zahurak, S. M.; Tycko, R.; Dabbagh, G.; Thiel, F. A., Conducting Films of C_{60} and C_{70} by Alkali-Metal Doping. *Nature* **1991,** 350, (6316), 320-322.

65. Hebard, A. F.; Rosseinsky, M. J.; Haddon, R. C.; Murphy, D. W.; Glarum, S. H.; Palstra, T. T. M.; Ramirez, A. P.; Kortan, A. R., Superconductivity at 18-K in Potassium-Doped C-60. *Nature* **1991,** 350, (6319), 600-601.

66. Baum, R., Fullerene Bioactivity - C-60 Derivative Inhibits Aids Viruses. *Chemical & Engineering News* **1993,** 71, (31), 3-4.

67. Iijima, S., Helical Microtubules of Graphitic Carbon. *Nature* **1991,** 354, (6348), 56-58.

68. Ishigami, M.; Cumings, J.; Zettl, A.; Chen, S., A simple method for the continuous production of carbon nanotubes. *Chem. Phys. Lett.* **2000,** 319, (5-6), 457-459.

69. Iijima, S.; Ichihashi, T., Single-Shell Carbon Nanotubes of 1-Nm Diameter. *Nature* **1993,** 363, (6430), 603-605.

70. Thess, A.; Lee, R.; Nikolaev, P.; Dai, H. J.; Petit, P.; Robert, J.; Xu, C. H.; Lee, Y. H.; Kim, S. G.; Rinzler, A. G.; Colbert, D. T.; Scuseria, G. E.; Tomanek, D.; Fischer, J. E.; Smalley, R. E., Crystalline ropes of metallic carbon nanotubes. *Science* **1996,** 273, (5274), 483-487.

71. Cassell, A. M.; Raymakers, J. A.; Kong, J.; Dai, H. J., Large scale CVD synthesis of single-walled carbon nanotubes. *J. Phys. Chem. B* **1999,** 103, (31), 6484-6492.

72. DeHeer, W. A.; Ugarte, D., Carbon Onions Produced by Heat-Treatment of Carbon Soot and Their Relation to the 217.5 Nm Interstellar Absorption Feature. *Chem. Phys. Lett.* **1993,** 207, (4-6), 480-486.

73. Lu, W.; Lieber, C. M., Semiconductor nanowires. *Journal of Physics D-Applied Physics* **2006,** 39, (21), R387-R406.

74. Huang, Y.; Duan, X. F.; Cui, Y.; Lauhon, L. J.; Kim, K. H.; Lieber, C. M., Logic gates and computation from assembled nanowire building blocks. *Science* **2001,** 294, (5545), 1313-1317.

75. Dimitrakopoulos, C. D.; Mascaro, D. J., Organic thin-film transistors: A review of recent advances. *IBM Journal of Research and Development* **2001,** 45, (1), 11-27.

76. Ugarte, D., Curling and Closure of Graphitic Networks under Electron-Beam Irradiation. *Nature* **1992,** 359, (6397), 707-709.

77. Banhart, F.; Fuller, T.; Redlich, P.; Ajayan, P. M., The formation, annealing and self-compression of carbon onions under electron irradiation. *Chem. Phys. Lett.* **1997,** 269, (3-4), 349-355.

78. Ugarte, D., Formation Mechanism of Quasi-Spherical Carbon Particles Induced by Electron-Bombardment. *Chem. Phys. Lett.* **1993,** 207, (4-6), 473-479.

79. Kuznetsov, V. L.; Chuvilin, A. L.; Butenko, Y. V.; Malkov, I. Y.; Titov, V. M., Onion-Like Carbon from Ultra-Disperse Diamond. *Chem. Phys. Lett.* **1994,** 222, (4), 343-348.

80. Cabioc'h, T.; Thune, E.; Riviere, J. P.; Camelio, S.; Girard, J. C.; Guerin, P.; Jaouen, M.; Henrard, L.; Lambin, P., Structure and properties of carbon onion layers deposited onto various substrates. *J. Appl. Phys.* **2002,** 91, (3), 1560-1567.

81. Chen, X. H.; Deng, F. M.; Wang, J. X.; Yang, H. S.; Wu, G. T.; Zhang, X. B.; Peng, J. C.; Li, W. Z., New method of carbon onion growth by radio-frequency plasma-enhanced chemical vapor deposition. *Chem. Phys. Lett.* **2001,** 336, (3-4), 201-204.

82. Sano, N.; Wang, H.; Chhowalla, M.; Alexandrou, I.; Amaratunga, G. A. J., Nanotechnology - Synthesis of carbon 'onions' in water. *Nature* **2001,** 414, (6863), 506-507.

83. Rettenbacher, A. S.; Elliott, B.; Hudson, J. S.; Amirkhanian, A.; Echegoyen, L., Preparation and functionalization of multilayer fullerenes (carbon nano-onions). *Chemistry-a European Journal* **2005,** 12, (2), 376-387.

84. Palkar, A.; Melin, F.; Cardona, C. M.; Elliott, B.; Naskar, A. K.; Edie, D. D.; Kumbhar, A.; Echegoyen, L., Reactivity Differences between Carbon Nano Onions (CNOs) Prepared by Different Methods. *Chemistry - An Asian Journal* **2007,** 0, (0), 0.

85. Muetterties, E. L.; Knoth, W. H., *Polyhedral Boranes*. Dekker: New York, 1968; p 197.

86. Wade, K., Structural and bonding patterns in cluster chemistry. *Advances in Inorganic Chemistry and Radiochemistry* **1976,** 18, 1-66.

87. Grimes, R. N., *Carboranes*. Academic: New York, 1970; p 272.

88. Muetterties, E. L. R., T. N.; Band, Elliot; Brucker, C. F.; Pretzer, W. R, Clusters and surfaces. *Chem. Rev.* **1979,** 79, 91-137.

89. Wheeler, R. G.; Laihing, K.; Wilson, W. L.; Allen, J. D.; King, R. B.; Duncan, M. A., Neutral Gas-Phase Analogs of Condensed-Phase Post-Transition-Metal Cluster Ions - Laser Vaporization and Photoionization of Sn/Bi and Pb/Sb Alloys. *J. Am. Chem. Soc.* **1986,** 108, (25), 8101-8102.

90. Wheeler, R. G.; Laihing, K.; Wilson, W. L.; Duncan, M. A., Growth-Patterns in Binary Clusters of Group-IV and Group-V Metals. *J. Chem. Phys.* **1988,** 88, (4), 2831-2839.

91. King, R. B., Chemical Bonding Topology of Bare Post-Transition-Metal Clusters - Analogies between Condensed-Phase and Gas-Phase Species. *J. Phys. Chem.* **1988,** 92, (15), 4452-4456.

92. Zintl, E., Intermetallic compounds. *Angew. Chem.* **1939,** 52, 1-6.

93. Belin, C.; Tillard-Charbonnel, M., Aspects of anionic framework formation. Clustering of p-block elements. *Coord. Chem. Rev.* **1998,** 178, 178-180.

94. Corbett, J. D., Diverse naked clusters of the heavy main-group elements. Electronic regularities and analogies. *Structural and Electronic Paradigms in Cluster Chemistry* **1997,** 87, 157-193.

95. Knight, W. D.; Clemenger, K.; Deheer, W. A.; Saunders, W. A.; Chou, M. Y.; Cohen, M. L., Electronic Shell Structure and Abundances of Sodium Clusters. *Phys. Rev. Lett.* **1984,** 52, (24), 2141-2143.

96. Knight, W. D.; Deheer, W. A.; Clemenger, K.; Saunders, W. A., Electronic Shell Structure in Potassium Clusters. *Solid State Commun.* **1985,** 53, (5), 445-446.

97. Bergeron, D. E.; Castleman, A. W.; Morisato, T.; Khanna, S. N., Formation of $Al_{13}I^-$: Evidence for the superhalogen character of Al_{13}^-. *Science* **2004,** 304, (5667), 84-87.

98. Bergeron, D. E.; Roach, P. J.; Castleman, A. W.; Jones, N.; Khanna, S. N., Al cluster superatoms as halogens in polyhalides and as alkaline earths in iodide salts. *Science* **2005,** 307, (5707), 231-235.

99. Kruis, F. E.; Fissan, H.; Peled, A., Synthesis of nanoparticles in the gas phase for electronic, optical and magnetic applications - A review. *J. Aerosol Sci.* **1998,** 29, (5-6), 511-535.

100. Guo, B. C.; Kerns, K. P.; Castleman, A. W., $Ti_8C_{12}^+$-Metallo-Carbohedrenes - a New Class of Molecular Clusters. *Science* **1992,** 255, (5050), 1411-1413.

101. Guo, B. C.; Wei, S.; Purnell, J.; Buzza, S.; Castleman, A. W., Metallo-Carbohedrenes [$M_8C_{12}^+$ (M = V, Zr, Hf, and Ti)] - a Class of Stable Molecular Cluster Ions. *Science* **1992,** 256, (5056), 515-516.

102. Wei, S.; Guo, B. C.; Purnell, J.; Buzza, S.; Castleman, A. W., Metallo-Carbohedrenes - Formation of Multicage Structures. *Science* **1992,** 256, (5058), 818-820.

103. Pilgrim, J. S.; Duncan, M. A., Beyond Metallo-Carbohedrenes - Growth and Decomposition of Metal-Carbon Nanocrystals. *J. Am. Chem. Soc.* **1993,** 115, (21), 9724-9727.

104. Pilgrim, J. S.; Duncan, M. A., Metallo-Carbohedrenes - Chromium, Iron, and Molybdenum Analogs. *J. Am. Chem. Soc.* **1993,** 115, (15), 6958-6961.

105. Pilgrim, J. S.; Duncan, M. A., Photodissociation of Metallo Carbohedrene (Met Cars) Cluster Cations. *J. Am. Chem. Soc.* **1993,** 115, (10), 4395-4396.

106. van Heijnsbergen, D.; von Helden, G.; Duncan, M. A.; van Roij, A. J. A.; Meijer, G., Vibrational spectroscopy of gas-phase metal-carbide clusters and nanocrystals. *Phys. Rev. Lett.* **1999,** 83, (24), 4983-4986.

107. von Helden, G.; Tielens, A. C. G. M.; van Heijnsbergen, D.; Duncan, M. A.; Hony, S.; Waters, L. B. F. M.; Meijer, G., Titanium carbide nanocrystals in circumstellar environments. *Science* **2000,** 288, (5464), 313-316.

108. Deng, H. T.; Guo, B. C.; Kerns, K. P.; Castleman, A. W., Gas-Phase Reactions of the Met-Cars $Ti_8C_{12}^+$, $Nb_8C_{12}^+$, and $Ti_7NbC_{12}^+$ with Acetone and Methyl-Iodide. *J. Phys. Chem.* **1994,** 98, (50), 13373-13378.

109. Cox, A., *Transition Metal Oxides*. Clarendon: Oxford, 1992.

110. Henrich, E.; Cox, A., *The Surface Science of Metal Oxides*. Cambridge University Press: Cambridge, 1994.

111. Rao, C. N.; Raveau, B., *Transition Metal Oxides*. Wiley: New York, 1998.

112. Somorjai, G. A., *Introduction to Surface Science and Catalysis*. Wiley Interscience: New York, 1994.

113. Hill, C. L.; Prossermccartha, C. M., Homogeneous Catalysis by Transition-Metal Oxygen Anion Clusters. *Coord. Chem. Rev.* **1995,** 143, 407-455.

114. Aiken, J. D.; Lin, Y.; Finke, R. G., A perspective on nanocluster catalysis: Polyoxoanion and $(n\text{-}C_4H_9N^+$ stabilized Ir(O) (similar to 300) nanocluster 'soluble heterogeneous catalysts'. *Journal of Molecular Catalysis a-Chemical* **1996,** 114, (1-3), 29-51.

115. Libuda, J.; Schalow, T.; Brandt, B.; Laurin, M.; Schauermann, S., Model studies in heterogeneous catalysis at the microscopic level: from the structure and composition of surfaces to reaction kinetics. *Microchimica Acta* **2006,** 156, (1-2), 9-20.

116. Ayers, T. M.; Fye, J. L.; Li, Q.; Duncan, M. A., Synthesis and isolation of titanium metal cluster complexes and ligand-coated nanoparticles with a laser vaporization flowtube reactor. *J. Cluster Sci.* **2003,** 14, (2), 97-113.

117. France, M. R.; Buchanan, J. W.; Robinson, J. C.; Pullins, S. H.; Tucker, J. L.; King, R. B.; Duncan, M. A., Antimony and bismuth oxide clusters: Growth and decomposition of new magic number clusters. *J. Phys. Chem. A* **1997,** 101, (35), 6214-6221.

118. van Heijnsbergen, D.; Demyk, K.; Duncan, M. A.; Meijer, G.; von Helden, G., Structure determination of gas phase aluminum oxide clusters. *Phys. Chem. Chem. Phys.* **2003,** 5, (12), 2515-2519.

119. van Heijnsbergen, D.; von Helden, G.; Meijer, G.; Duncan, M. A., Infrared resonance-enhanced multiphoton ionization spectroscopy of magnesium oxide clusters. *J. Chem. Phys.* **2002,** 116, (6), 2400-2406.

120. *Clusters of Atoms and Molecules II*. Springer-Verlag: Berlin, 1994; Vol. 56.

121. *Clusters of Atoms and Molecules I*. 2nd ed.; Springer-Verlag: Berlin, 1995; Vol. 52.

122. Molek, K. S.; Jaeger, T. D.; Duncan, M. A., Photodissociation of vanadium, niobium, and tantalum oxide cluster cations. *J. Chem. Phys.* **2005,** 123, (14), -.

123. von Helden, G.; Kirilyuk, A.; van Heijnsbergen, D.; Sartakov, B.; Duncan, M. A.; Meijer, G., Infrared spectroscopy of gas-phase zirconium oxide clusters. *Chem. Phys.* **2000,** 262, (1), 31-39.

124. von Helden, G.; van Heijnsbergen, D.; Meijer, G., Resonant ionization using IR light: A new tool to study the spectroscopy and dynamics of gas-phase molecules and clusters. *J. Phys. Chem. A* **2003,** 107, (11), 1671-1688.

125. Deshpande, M.; Kanhere, D. G.; Pandey, R., Structural and electronic properties of neutral and ionic Ga_nO_n clusters with n=4-7. *J. Phys. Chem. A* **2006,** 110, (10), 3812-3813.

126. Gowtham, S.; Costales, A.; Pandey, R., Theoretical study of neutral and ionic states of small clusters of Ga_mO_n (m, n = 1, 2). *J. Phys. Chem. B* **2004,** 108, (45), 17295-17300.

127. Gowtham, S.; Deshpande, M.; Costales, A.; Pandey, R., Structural, energetic, electronic, bonding, and vibrational properties of Ga_3O, Ga_3O_2, Ga_3O_3, Ga_2O_3, and GaO_3 clusters. *J. Phys. Chem. B* **2005,** 109, (31), 14836-14844.

128. He, H. Y.; Orlando, R.; Blanco, M. A.; Pandey, R.; Amzallag, E.; Baraille, I.; Rerat, M., First-principles study of the structural, electronic, and optical properties of Ga_2O_3 in its monoclinic and hexagonal phases. *Physical Review B* **2006,** 74, (19).

129. King, F. L.; Dunlap, B. I.; Parent, D. C., Characterization of Cluster Ions Produced by the Sputtering or Direct Laser Vaporization of Group-13 Metal (Al, Ga, and In) Oxides. *J. Chem. Phys.* **1991,** 94, (4), 2578-2587.

Table 1.1. This shows the number of electrons in different shells of the spherical Jellium model

Energy Levels	**Number of Electrons**
1s	2
1p	6
1d	10
2s	2
1f	14
2p	6

FIGURES

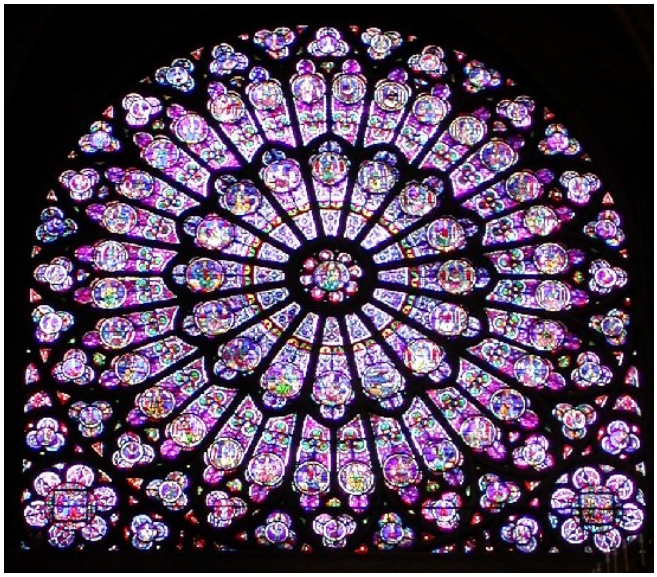

Figure 1.1. Rose window in the cathedral of Notre Dame. The bright red color is the result of surface plasmon resonances in colloidal gold nanoparticles.

Figure 1.2. Cave paintings in Lascaux, France. The bright colors result from colloidal gold nanoparticles.

CHAPTER 2

EXPERIMENTAL

2.1 LASER DESORPTION APPARATUS

The laser desorption time-of-flight mass spectrometer (TOF-MS) used in these experiments has been described previously.[1] It has the capability for high acceleration fields (up to 30 kV) and delayed pulsed extraction for improved resolution.[2] A diagram of the instrument is presented in Figure 2.1. A 4.8 mm stainless steel probe is employed for the mounting of samples. Samples can be prepared by mixing powders with a mortar and pestle or a spatula and then pressing them onto the probe tip; by putting the sample in a solvent to make a slurry and adding the slurry dropwise to the probe tip; or by packing the sample into a hollow probe tip. Sodium and potassium are present as impurities resulting from the handling of samples. However, these can aid in the assignment of spectra by providing regular, known, reference masses. Smooth sample surfaces are essential to obtain the best results in these laser desorption experiments. Once prepared, the samples are inserted into the mass spectrometer for analysis. The laser may vaporize atoms in the sample where they collide and grow in the plasma or desorb molecules or compounds directly into the gas phase.

Laser vaporization techniques for cluster production and analysis have been in use for some time.[2-4] Vaporization, ionization, and cluster growth are accomplished by focusing the laser onto the sample in the probe tip inside the mass spectrometer. The fluence of the laser is adjusted with a variable attenuator prior to focusing in order to optimize production of the desired clusters. This ensures that energies less than 1 mJ/pulse are employed for most of these experiments. Unlike molecular beam experiments, a collisional cooling gas is not used for cluster production. Rather, clusters grow and are ionized due to ion/molecule reactions in the laser-induced plasma.[5] While the plasma environment is not well understood, some characteristics of it are known. It consists of ions, neutral atoms, and electrons interacting and

colliding with high energy. Three-body collisions may cause clusters to grow in the plasma, while laser desorption and collisional ionization of clusters already in existence is also possible. The system determines which trends predominate. Growth of larger clusters is enhanced after the laser has formed a channel in the sample. Ion/molecule reactions occur better there before the ions expand into the low pressure source.[5] While ion/molecular reactions in the plasma grow clusters, collision-induced dissociation reactions can break down clusters. Larger clusters may break apart into more stable clusters in these experiments.[140]

The clusters that grow in the plasma have been observed to exhibit nonstatistical distributions of atoms or "magic numbers." While it is difficult to unambiguously determine the basis for these nonstatistical distributions, magic numbers, as in the case of C_{60}, may imply special structural or electronic properties that provide greater stability for the cluster. However, the dynamics of the experimental apparatus and the method of cluster production and measurement play an important role in the cluster distribution seen and in the supposed stability of the clusters. Because clusters must exist as ions to be detected in our experiment, several complications in terms of stability measurement are introduced. 1) Collisional growth kinetics and dynamics. Magic numbers seen are the result of collisional cluster growth and the step-by-step addition of more and more atoms. Highly unstable intermediates to larger stable clusters could act as a bottleneck in cluster growth; bottlenecks could prevent larger stable clusters from being formed. 2) Ionization energies. To be detected, the cluster formed must be able to be ionized by the energy introduced by our 532 nm Nd:YAG laser. A stable cluster with an exceptionally high IP may not be seen as a magic number in our experiments. 3) Cluster fragmentation. If one atom collided with a larger cluster, several atoms could fragment off if one of the resulting clusters was extremely stable. This would result in a misleading distribution of

large cluster stability. Plasma, collisional, ionization, and fragmentation dynamics and kinetics play large roles in the magic numbers seen. Since all of these processes are not completely understood, direct stability measurement is difficult.

Once the material vaporizes and possibly reacts in the plasma, the clusters are accelerated down the flight tube by an electric field generated from a repeller plate. The energy of the clusters is determined by the voltage on the plates and the kinetic energy theorem as shown by the equation,

$$KE = zeV = 1/2\ mv^2 \quad (1)$$

where KE is the kinetic energy, z is the charge of the particle, *e* is the elementary charge constant ($1.602*10^{-19}$ C), *V* is the electric field strength, m is the mass of the particle and v is the velocity of the particle. Using v=d/t, this equation can be solved to show that the time of flight of the ion is proportional to the square root of its mass-to-charge ratio (*m/z*). After being accelerated, the ions are focused with an einzel lens before reaching the detector. The flight time is measured from when the laser fires to when the clusters collide with the detector. Mass to charge ratios are calibrated using known flight times for reference masses. Mass spectra are collected at 10 Hz, and 30-300 shots are generally averaged with a digital oscilloscope (LeCroy LT 341) and transferred to a PC via an IEEE-488 interface for processing.

2.2 BRUKER AUTOFLEX MASS SPECTROMETER

The Bruker Autoflex mass spectrometer is a commercial instrument available through The University of Georgia's chemical sciences mass spectrometry facility.[6] It functions similar to the above apparatus but has several important differences. Rather than one sample being inserted on a probe tip, multiple samples are introduced using a stainless steel block. Desorption and ionization is accomplished by focusing a nitrogen laser onto the sample. The fluence of the

laser is adjusted internally, and energies of 10-20 μJ, which are far less than those from the YAG laser, are used. Small particles with high IP's are ionized better using a higher-powered laser to generate a higher-energy plasma. However, the low powered laser is advantageous for large particles such as carbon onions because it ionizes them without fragmenting them. Another important difference in the Bruker instrument is that clusters can be post-accelerated just before they reach the detector using a "turbo" feature so that high mass clusters are detected better. This feature consists of pulsed acceleration plates that switch from ground to charged after the desired particles pass them. In this way, they are given more kinetic energy than is possible from just the repeller plates, which are limited to voltages of less than 30 kV. This dual acceleration system is advantageous because soft, slow, high mass particles that hit the detector may deform and inefficiently eject electrons as they collide with the electron multiplier tube (EMT) detector. High mass particles with greater velocities are detected better. Thus, the Bruker instrument is better for analysis of high mass particles because it uses a nitrogen laser and a post-acceleration plate.

2.3 REFERENCES

1. Cornett, D. S.; Amster, I. J.; Duncan, M. A.; Rao, A. M.; Eklund, P. C., Laser Desorption Mass-Spectrometry of Photopolymerized C-60 Films. *J. Phys. Chem.* **1993,** 97, (19), 5036-5039.

2. Wiley, W. C.; Mclaren, I. H., Time-of-Flight Mass Spectrometer with Improved Resolution. *Rev. Sci. Instrum.* **1955,** 26, (12), 1150-1157.

3. *Clusters of Atoms and Molecules I*. 2nd ed.; Springer-Verlag: Berlin, 1995; Vol. 52.

4. Dietz, T. G.; Duncan, M. A.; Powers, D. E.; Smalley, R. E., Laser Production of Supersonic Metal Cluster Beams. *J. Chem. Phys.* **1981,** 74, (11), 6511-6512.

5. McElvany, S. W.; Nelson, H. H.; Baronavski, A. P.; Watson, C. H.; Eyler, J. R., FT-MS Studies of Mass-Selected, Large Cluster Ions Produced by Direct Laser Vaporization. *Chem. Phys. Lett.* **1987,** 134, (3), 214-219.

6. Bruker Daltonics, I., 2007; Vol. 2007.

FIGURES

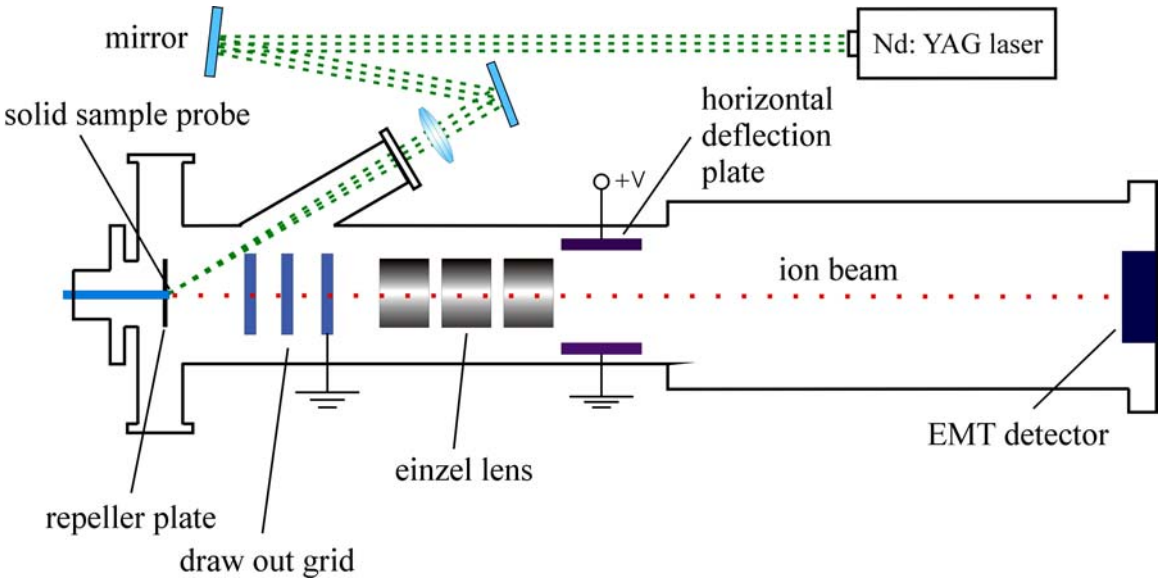

Figure 2.1. A diagram of the Duncan lab laser desorption time-of-flight mass spectrometers used in these experiments.

CHAPTER 3

METAL SULFUR CLUSTERS[1]

1. Ham, P.B.; Ayers, T.M.; Duncan, M.A. To be submitted to *International Journal of Mass Spectrometry.*

3.1 BACKGROUND

The study of nanoparticles is currently an area of intense interest because they have applications in areas such as surface science, biology, catalysis, and nanocircuits.[1-3] Like nanoparticles, metal clusters have optical properties, reactivity, catalytic chemistry, and other properties that differ significantly from the bulk.[2, 4, 5] Alloy and metal compound nanoparticles also have unique chemical and physical properties. Aluminum, gallium, and indium sulfur clusters are an example of metal compound clusters that may have applications, be similar to metal oxides, and form clusters that can be modeled by electron counting rules.

Because of their potential applications, numerous studies on metal sulfur clusters have been performed. Metal sulfur clusters exist at metalloprotein active sites,[6] and these systems play important roles in catalysis and as semiconductors.[7] Despite their importance, only a few gas phase metal sulfur cluster systems have been previously studied. Transition metal sulfur clusters have been studied previously, particularly iron sulfur clusters.[8] Dance and coworkers investigated gas phase lanthanide sulfur cluster chemistry and they found sequential additions of S_8 rings to LaS_3^+.[9] Carbon and other sulfur clusters have been investigated and magic numbers noted.[10] Other studies have focused on aluminum sulfide anions in which sequential additions of Al_2S_3 to a base of AlS^- were noted.[11, 12] Also, aluminum sulfur cations measured with a time of flight mass spectrometer had mass distributions of $AlS^+(Al_2S_3)_n$ where n = 1,2,3,...,31.[13] However, no comparative study of aluminum, gallium, and indium sulfur clusters has been performed.

Based on oxidation states, metal sulfur clusters are expected to be similar to metal oxide clusters. Metal oxide clusters, known for their catalytic properties, have been investigated previously.[14-22] The IP's of metal oxide clusters have been determined by charge transfer[23]; structures have been determined using density functional theory (B3LYP)[24]; and photoelectron

spectra have been measured.[24] Also, the mass spectra of Zr, Ti, Mg, and Al oxides have been measured. [19, 20, 25, 26] In the mass spectra, aluminum oxide clusters are observed in nonstatistical distributions of the form $AlO^{+}(Al_2O_3)_n$. This is the same pattern observed with aluminum sulfide clusters![11-13] Gallium oxide clusters have also been studied.[27-31] Mass spectrometry[31] and theoretical methods[27-30] have been used to investigate gallium oxide clusters and determine structures. Furthermore, indium oxide clusters have been investigated for their potential use as semiconductors. Their structures were determined using electronic structure calculations,[32] and materials with a larger amount of indium were found to exhibit a more favorable band gap. [33] These studies observed that the prevalence of certain ions in the metal oxide mass spectra was not merely a statistical fluctuation; the structure and electronic arrangement of the ions determine their stability in the gas phase. Because sulfur is in the same group as oxygen, metal sulfur clusters are expected to have similar properties and may exhibit nonstatistical combinations in our experiments.

Aluminum, gallium, and indium sulfur clusters are especially appealing because they may form clusters that can be modeled by electron counting rules.[34] Aluminum, gallium, and indium sulfides may form Wade's rules clusters if they are electron deficient. The polyhedral skeletal electron pair theory, known colloquially as “Wade’s rules,” predicts structure and stability for certain kinds of electron deficient clusters.[35] They are famous for predicting the structure and stability of borane,[36, 37] carborane,[38] and metal carbonyl clusters.[39] For a polyhedron with N atoms, increased stability is expected for clusters with 2N+2, 2N+4, and 2N+6 skeletal electrons. These are denoted closo, nido, and arachno, respectively, for their relevance to cluster shape and structure. The enhanced stability is due to a type of 3D aromaticity; since not enough electrons are available to satisfy all of the atoms, the p orbitals of the constituent atoms point towards the center of the cluster

where they share electron density.[40-42] The nido and arachno forms have open faces where the shared electron density is exposed. These are a potential binding site for other elements. Some condensed phase clusters similar to metal sulfur clusters that satisfy these rules are the "Zintl" ions. Zintl found that condensed-phase metal clusters of Sn_5^{2-}, Pb_5^{2-}, Pb_9^{4-}, Bi_9^{5+}, and Ge_9^{4-} form when these metals are dissolved in liquid ammonia.[43] While these clusters were known to be stable, it was not initially known why. It was discovered much later that these clusters satisfied Wade's rules.[44, 45] Later, heteroatomic clusters of Sn/Bi and Pb/Sb were produced in the gas phase that were isoelectronic to the condensed phase Zintl ions.[40, 41] These multielemental clusters satisfied Wade's rules. Other multielemental clusters have also been found, including those with group 13 elements.[46, 47] The Zintl phases of the group 13 elements Ga, In, and Tl have been studied in the condensed phase with alkali metals and Bi[48, 49]; aluminum, gallium, and indium are generally electron deficient in binding. Thus, when combined with a limited number of sulfur atoms, they could form clusters satisfying Wade's rules. However, the amount of s and p orbital energy separation is greater in the heavier elements. Aluminum is expected to exhibit different properties than indium because it can use both its s and p orbitals in bonding. Gallium is expected to be an intermediate case. Thus, if group 13 element clusters with sulfur are found to be prevalent in mass spectra and correspond to Wade's electron counting rules, this can have important implications for their structure and can suggest enhanced stability in the condensed phase.

While electron poor species may form Wade's rules clusters, electron rich species may form spherical Jellium clusters. Jellium clusters are "superatoms" that have interacting electrons in a uniform background of positive charge like blobs of jelly, hence the name. These interacting electrons are organized into super-atom orbitals similar to the organization of electrons in atoms. The orbitals are organized into valence shells with observed valence shell closings at 8, 20, 40, and

58 electrons.[50, 51] This phenomena was first observed with clusters of sodium[51] and potassium.[50] Like normal atoms, superatoms are most stable when they have a closed shell of electrons in this new counting scheme. Therefore, superatoms with more electrons than a full shell, like an alkali or alkaline metal, lose that electron very easily while superatoms with more than a full shell of electrons, like a halogen, should have a large electron affinity.[52, 53] Studies of pure aluminum, gallium, and indium clusters were found to follow the Jellium model, although gallium was, for the most part, irregular.[54-56] Aluminum cluster IP measurements suggest possible shell closings at Al_3^+, Al_7^+, Al_{13}^-, and also at 22 and 66 atoms.[54] Indium measurements suggest shell closings at 47, 66, and 112 atoms[56] while gallium suggested a shell closing at Ga_7^+.[57] These values correspond with Jellium model predictions.[58, 59] However, Jellium irregularities in clusters of these elements have been attributed to crystal field splittings and sp hybridization effects.[59, 60] In larger clusters of these elements, a transition to metallic bonding was observed between 15 and 30 atoms as suggested by IP measurements.[60] Clusters that do not follow the Jellium model or Wade's rules may exhibit valence bonding or follow some other bonding model.

In this paper, we investigated aluminum, gallium, and indium sulfides. First, we measured mass spectra using a laser desorption mass spectrometer. Then, we found patterns in the distributions of clusters and explained these patterns using bonding models.

3.2 EXPERIMENTAL

The laser desorption time-of-flight mass spectrometer (TOF-MS) used in these experiments has been described previously.[61] It has the capability for high acceleration fields (up to 30 kV) and delayed pulsed extraction for improved resolution.[62] A 4.8 mm stainless steel probe is employed for the mounting of solid samples of aluminum, gallium, and indium powders mixed with sulfur powder. The sample consists of well mixed Al, Ga, or In powder from Aldrich

or Alfa Aesar and precipitated sulfur powder, each of purity greater than 99%. The powders are mixed using a mortar and pestle or a spatula and then pressed onto the probe tip. Sodium and potassium are present as impurities resulting from the handling of samples. However, these can aid in the assignment of spectra by providing regular, known, reference masses. Smooth sample surfaces are essential to obtain the best results in these laser desorption experiments. Once prepared, the samples are inserted into the mass spectrometer for analysis. The low vapor pressure of the metals and sulfur allows the sample to reside in a vacuum for an indefinite period of time without being pumped away. All chemicals are used as received without further purification.

Vaporization and ionization are accomplished by focusing (20 cm lens) the second harmonic of an Nd:YAG laser (Continuum Minilite 532 nm) onto the sample in the probe tip inside the mass spectrometer. The fluence of the laser is adjusted with a variable attenuator prior to focusing in order to optimize production of the desired clusters. This ensures that energies less than 1 mJ/pulse are employed for most of these experiments. Once the material is vaporized, cations are accelerated down the flight tube at an energy of 10 keV and focused with an einzel lens before reaching the detector. Mass spectra are collected and averaged with a digital oscilloscope (LeCroy LT 341) and transferred to a PC via an IEEE-488 interface for processing.

3.3 RESULTS

In Figure 3.1, spectra of aluminum sulfur clusters are presented. These spectra were difficult to assign because the mass difference between aluminum (27 amu) and sulfur (32 amu) is only 5 amu and sulfur has an isotope at 34 amu that is 4% abundant. Therefore, as seen in Table 3.1, several assignments are possible, particularly at high masses. Those deemed most

probable by comparison with other experiments are labeled in the actual spectra. The largest clusters form only when the molar sulfur concentration is at least three times greater than the aluminum concentration as seen in the top graph. When the sulfur concentration is lower, as seen in the next two parts of the figure, only the smaller clusters form. The lowest mass clusters are of the form $Al_1S_m^+$, where m=3-10. The high mass aluminum sulfur clusters are of the form (1) $Al_3S_1^+$ + (1) S_8 + (n) Al_2S_3, where (1) implies that the cluster has only one of that type of stoichiometry added, and (n) implies the constituent has varying amounts added. In this case, (n) varies from one to four. The smaller peaks to the left of the larger peaks generally have a mass difference of five atomic mass units. Since the mass of sulfur and aluminum is five atomic mass units apart, the smaller peaks have one less sulfur and one more aluminum atom. The lowest S/Al ratio figure also has a few peaks that are more noticeable than in the other spectra. It has Al_3^+, Al_4^+, $Al_3S_1^+$, $Al_1S_3^+$ (not labeled), $Al_2S_3^+$, and $Al_1S_4^+$.

Figure 3.2 presents two spectra of gallium sulfur clusters that we obtained. The bottom gallium sulfur mass spectrum shows prominent peaks of $Ga_3S_1^+$, $Ga_3S_2^+$, and $Ga_5S_4^+$ for the experiment where sulfur was introduced in low relative concentration. The $Ga_3S_1^+$ peak is the most dominant peak in the spectrum, and its integrated area is greater than that of the $Ga_3S_2^+$ peak. However, in the higher relative sulfur concentration experiment, the $Ga_3S_1^+$ peak is nearly equivalent to the $Ga_3S_2^+$ peak. Also in the high concentration experiment, a $Ga_3S_6^+$, a $Ga_5S_3^+$, and a $Ga_3S_9^+$ peak have appeared and the sulfur distribution, S_n^+ where n=2-5, is readily visible.

High and low sulfur spectra of indium sulfur clusters were also obtained and are presented in Figure 3.3. The most prevalent cluster species formed follow several patterns. The largest indium and indium sulfur peaks in the spectra all have an odd number of atoms. The prominent indium sulfur peaks are $In_3S_1^+$, $In_5S_3^+$, $In_7S_5^+$, $In_9S_7^+$and $In_{11}S_9^+$. All of these have

two less sulfur atoms (s) than indium atoms (n). So the general stoichiometry for these clusters is s=n-2. The second most prominent indium sulfur peaks are $In_3S_2^+$, $In_5S_4^+$, $In_7S_6^+$, $In_9S_8^+$, and $In_{11}S_{10}^+$. They also have one less sulfur atom than indium atoms. So, the general stoichiometry for these clusters is s=n-1. The preference for the n-2 clusters becomes less and less as the clusters grow. In fact, the $In_{11}S_{10}^+$ cluster is actually slightly higher than the $In_{11}S_9^+$ cluster. These are the trends that dominate the high sulfur concentration indium sulfur mass spectrum.

In the low sulfur concentration spectrum, none of the larger clusters are formed. Also notable in the indium spectrum is that the $In_3S_1^+$ cluster has a significantly greater integrated area than the $In_3S_2^+$ cluster, as in the gallium sulfur spectrum. In addition, no peaks are visible for $In_3S_9^+$. The sulfur distribution is visible in the high sulfur concentration spectrum, and In_3^+ is visible in the low concentration spectrum. Mass spectra for sulfur clusters, aluminum clusters, and indium clusters, are presented in Figures 3.4-3.6. Large metal clusters are not seen in abundance in these experiments. Few metal oxides are observed in these spectra. They appear in greater abundance when the metal is mixed with acid. This is of critical importance because mass coincidences occur between sulfur (32 amu) and oxygen (16 amu).

3.4 DISCUSSION

Each of the spectra produced (Figures 3.1-3.3) has a nonstatistical distribution of clusters. Thus, factors that could affect the stability of a cluster such as known bonding schemes, aromaticities, special structures, and electron counting rules can be utilized to try to elucidate the reasons behind the nonstatistical distributions.

3.4.1 ALUMINUM SULFUR

The aluminum sulfur spectrum can be explained using valence bonding ideas, bulk stoichiometry logic, and ideas about the collisional growth of clusters in plasmas. Valence

bonding ideas can explain the $Al_1S_m^+$ peaks if they are modeled as sulfur rings with an aluminum atom substitute. This satisfies the valence of sulfur and the charge is located on aluminum. Previously gas phase sulfur cluster experiments have suggested the importance of S_8 rings, although in the condensed phase, more than 30 other allotropes of sulfur exist including smaller and larger rings.[63-65] Many other unlabeled peaks in the spectra with high sulfur content can also be explained by valence bonding. The cluster $Al_3S_1^+$ can be explained by valence bonding ideas if the aluminum atoms are all bonded to the sulfur atom. The p^1 electrons of the three aluminum atoms could form bonds with the sulfur; this gives sulfur one more bond than desired and a 1+ charge, which corresponds to the overall charge of the cluster as shown below.

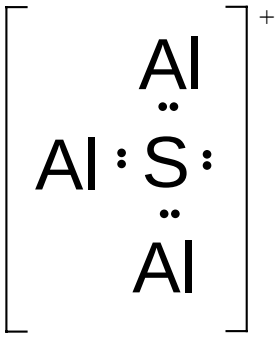

However, this structure is sensible only if the *p* electrons are considered for aluminum.

Furthermore, it is interesting that the $Al_3S_1^+$ cluster does not have the same intensity relative to the other peaks when the low and high sulfur concentration spectra are compared. Since 1) the cluster $Al_3S_9^+$ has a very high intensity in the high sulfur concentration spectra, 2) S_8 rings are a stable form of sulfur, and 3) cluster growth occurs in plasmas by three body collisions, this implies that one growth pathway to the $Al_3S_9^+$ cluster may be through a collision between $Al_3S_1^+$, S_8, and another particle. $Al_3S_1^+$ and S_8 may bond, and the other particle speeds away with the extra kinetic energy from the bond formation. Since the $Al_3S_1^+$ cluster has a positive charge and S_8 rings have two lone pairs on every atom and filled d orbitals, the lone pair

and d orbital electrons may have an electrostatic attraction to the charged cluster. Other experiments confirm this as a possibility. Dance and coworkers observed S_8 ring additions with lanthanide sulfur cluster cations and lanthanum has the same +3 oxidation state as aluminum.[9] This collisional cluster growth model may also apply to other clusters reported. Similar logic can explain the $Al_5S_{12}^+$ peak and higher mass peaks. If a three-body collision between a neutral molecule having the bulk stoichiometry Al_2S_3, the $Al_3S_9^+$ cluster, and another particle occurred, then the $Al_5S_{12}^+$ cluster could be formed. Also, differences of M_2S_3 and M_2O_3 have been noted previously in metal sulfur spectra and metal oxide mass spectra.[11-13, 31, 66, 67] However, this is the first time that both have been noted in a single experiment. Thus, stable clusters seen in mass spectra may be building blocks for the growth of larger clusters by the subsequent addition of S_8 and Al_2S_3. It is interesting that previous aluminum sulfur experiments observe a base of AlS^+ to which Al_2S_3 adds.[13] One reason for this discrepancy could be that they used a 248 nm laser in their experiments while we used a 532 nm laser in ours. Since larger clusters are typically easier to ionize than smaller clusters, the AlS^+ cluster may not be ionized in our experiments. The AlS^+ trend was also not observed when these experiments were performed with a 355 nm laser.

Electron counting rules can be used to explain other peaks in the spectra. Wade's rules apply to the $Al_1S_3^+$ and $Al_1S_4^+$ clusters as summarized in Table 3.2. Aluminum has 1 p electron and sulfur has 4 p electrons. Therefore, the $Al_1S_3^+$ cluster has 12 valence electrons. This satisfies the 2n+4 nido form of Wade's rules. Thus, the structure for it may be a deltahedron with an open side. The $Al_1S_4^+$ cluster has 16 valence electrons and satisfies the 2n+6 arachno form of Wade's rules. Thus, the structure for it may be a deltahedron with two open sides. Also, as suggested previously, Al_3^+ could be a Jellium cluster. It has eight electrons, which closes the 1p

Jellium shell, although the Al_7^+ peak is usually much bigger.[53, 54] Thus, all clusters observed can be explained using condensed phase bonding ideas.

3.4.3 GALLIUM SULFUR

Like the aluminum case, the prevalence of gallium sulfur clusters can also be explained using valence bonding ideas, bulk stoichiometry logic, and ideas about the collisional growth of clusters in plasmas. Since the $Ga_3S_1^+$ peak is the most dominant peak in the low sulfur concentration spectrum and it is nearly equivalent to the $Ga_3S_2^+$ peak in the low concentration spectrum, either less $Ga_3S_1^+$ was produced in the higher sulfur concentration experiment or a substantial amount of $Ga_3S_1^+$ was preferentially consumed in reactions with other species in the plasma. Like the aluminum case, the latter is more probable because $Ga_3S_1^+$ could also react with an S_8 ring to form a structure with three gallium atoms and nine sulfur atoms–precisely what is observed in the high sulfur concentration mass spectrum but not observed in the low sulfur concentration spectra. $Ga_3S_1^+$ could have a similar structure to that suggested for aluminum sulfur above. In Figure 3.2, however, the results are clearer than the aluminum spectra because there are less peaks. Other sulfur rings could also add to stable clusters. For example, if an S_5 fragment added to the $Ga_3S_1^+$ cluster, it would produce $Ga_3S_6^+$, a peak also seen in the spectrum. Additionally, if Ga_2S_3 added to $Ga_3S_1^+$, it would produce a cluster with a $Ga_5S_4^+$, a stoichiometry seen in both spectra. For the Ga_2S_3 cluster, counting p valence electrons of sulfur and s and p valence electrons of gallium, 18 electrons are added to the system. Other alternate explanations are also possible. For example, the $Ga_5S_4^+$ stoichiometry satisfies the closo form of Wade's rules. This could give the cluster a different structure from one produced by the reaction of $Ga_3S_1^+$ with Ga_2S_3. The $Ga_5S_4^+$ structure satisfying Wade's rules would exist as a tricapped trigonal prism.

3.4.3 INDIUM SULFUR

While some of the indium sulfur clusters produced can be explained by valence bonding, none can be explained using bulk logic, and the majority can be explained by Wade's rules. Simple valence bond models can be drawn for the $In_3S_1^+$ and $In_3S_2^+$ clusters. Also notable in the indium spectrum is that that no peaks are visible for $In_3S_9^+$. If S_8 does not add to the $In_3S_1^+$ cluster, then no $In_3S_9^+$ is formed, no $In_3S_1^+$ is consumed in reaction, and the $In_3S_1^+$ cluster should be present in larger amounts. This is indeed the case. It has a significantly greater integrated area than the $In_3S_2^+$ cluster, as in the low sulfur concentration gallium sulfur spectrum. This implies that as the clusters are composed of heavier and heavier atoms, different trends begin to predominate. The $In_3S_1^+$ cluster may not have its charge easily accessible for bonding since indium atoms are larger than aluminum and gallium atoms. In addition, the s-p orbital energy difference is greatest in indium and least for alumimum. This means that the s and p orbitals will not mix as easily and that the p orbitals will be more available for binding than the s orbitals. Therefore, for the $In_3S_1^+$ cluster, it is much more likely than aluminum to have the structure suggested below where the s electrons do not participate.

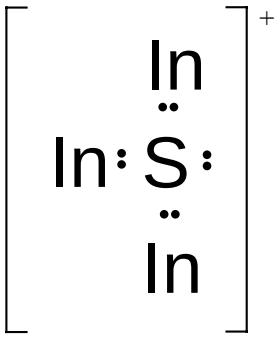

Theory and experimental studies by Schleyer, et al. for the oxide analog of this species, $In_3O_1^+$, has shown that the neutral cluster has a very low IP and that $In_3S_1^+$ is a very stable cation.[68] Since sulfides are comparable to oxides, this is likely to be the reason it is observed in such high

abundance. The $In_3O_1^+$ oxide cluster's calculated structure is very similar to that suggested above for aluminum. Furthermore, in the indium sulfur spectra, Wade's rule clusters dominate more than in the aluminum sulfur spectra and the gallium sulfur spectra. Indium sulfur clusters that satisfy Wade's rules are summarized in Table 3.1. Wade's rules structures seem to explain the stoichiometric distributions of many of these clusters. This also makes sense because of the p orbital spacing. For example, the $In_7S_5^+$ cluster has 12 total atoms, 26 p electrons, and satisfies the closo form of Wade's rules. A 12 atom closo Wade's rules structure would have an icosahedral structure. The other cluster structures are derived similarly. However, this evidence does not prove the structures of these clusters–it only suggests them. IR spectroscopy, theoretical investigations, and X-ray crystallography could be useful to further investigate their structures. Additionally, it is interesting that at the point that Wade's rules no longer apply because of the many sulfur atoms, other peaks become as prevalent as the n-2 and n-1 peaks seen to dominate the lower mass clusters.

3.4.4 SUMMARY

Several observations about all systems are also notable. First, metal atoms were present in the largest quantities with an odd number of atoms. This implies that few or no singly charged radical species were stable in the experiment. Second, in the low sulfur concentration spectra, larger metal sulfur clusters are not formed. This implies that sulfur may be needed for the large clusters to grow. Third, because high mass species do not form in the pure metal cluster experiments, it is not likely that the clusters exist with a large metal to sulfur ratio. Large clusters that are difficult to identify in the aluminum sulfur spectra likely do not have substantially more metal than sulfur. Fourth, oxides are not present in large amounts because observed metal oxide peaks of $AlO^+(Al_2O_3)_n$ do not occur in the metal sulfur experiments. If

metal oxides were present, every other metal oxide peak would fall under a possible metal sulfur peak, but the remainder should not. The other peaks are not visible in these spectra. The pure metal experiments as shown in Figures 3.4-3.6 do not have large metal oxide peaks. Oxide contamination is unlikely as well because no low mass aluminum oxide peaks are seen in the high concentration aluminum sulfur spectrum. If oxides are present in substantial amounts, peaks would be observed at 70 amu and at 97 amu as in Figure 3.5. These peaks are not observed in Figure 3.1.

3.5 CONCLUSIONS

Aluminum, gallium and indium sulfur clusters have similar trends in bonding. However, gallium sulfur is slightly different than aluminum sulfur, and indium sulfur is slightly different than gallium sulfur. Sulfur clusters with aluminum appear to be based off of an $Al_3S_1^+$ cluster that sequentially adds units of one S_8 and multiple Al_2S_3 clusters. Gallium is a combined case of aluminum and indium, which is reasonable because of its intermediate size, nuclear charge, electronegativity, and electronic properties. It also has the $Ga_3S_1^+$ unit that satisfies the nido form of Wade's electron counting rules and sequentially adds one S_8 unit. However, no sequential additions of Ga_2S_3 were observed to the Ga_3S_9 cluster. The $Ga_5S_4^+$ unit satisfies Wade's rules, but could also result from the addition of Ga_2S_3 to the $Ga_3S_1^+$ unit. The indium sulfur system has the most clusters that satisfy Wade's rules, and it does not seem to exhibit the sequential addition ability of either aluminum or gallium. Wade's rules can be utilized with other electron counting rules to explain the intensities of noted peaks. Structural stability gained through 3D aromaticity can account for the nonstatistical distributions, again showing that condensed phase electron counting rules can be applicable in the gas phase as well.

3.6 REFERENCES

1. Bruchez, M.; Moronne, M.; Gin, P.; Weiss, S.; Alivisatos, A. P., Semiconductor nanocrystals as fluorescent biological labels. *Science* **1998,** 281, (5385), 2013-2016.

2. Daniel, M. C.; Astruc, D., Gold nanoparticles: Assembly, supramolecular chemistry, quantum-size-related properties, and applications toward biology, catalysis, and nanotechnology. *Chem. Rev.* **2004,** 104, (1), 293-346.

3. Klabunde, K. J., *Nanoscale Materials in Chemistry*. John Wiley and Sons, Inc.: New York, 2004.

4. Brust, M.; Walker, M.; Bethell, D.; Schiffrin, D. J.; Whyman, R., Synthesis of Thiol-Derivatized Gold Nanoparticles in a 2-Phase Liquid-Liquid System. *J. Chem. Soc. Chem. Comm.* **1994**, (7), 801-802.

5. Kim, M. K.; Jeon, Y. M.; Jeon, W. S.; Kim, H. J.; Kim, K.; Hong, S. G.; Park, C. G., Novel dendron-stabilized gold nanoparticles with high stability and narrow size distribution. *Chem. Comm.* **2001,** 7, 667.

6. Webster, C. E.; Darensbourg, M. Y.; Lindahl, P. A.; Hall, M. B., Structures and energetics of models for the active site of acetyl-coenzyme a synthase: Role of distal and proximal metals in catalysis. *J. Am. Chem. Soc.* **2004,** 126, (11), 3410-3411.

7. Stiefel, E. I.; Matsumoto, K., *Transition Metal Sulfur Chemistry*. American Chemical Society: Washington, DC, 1996.

8. Shi, Y.; Yu, Z. D.; Zhang, N.; Gao, Z.; Kong, F. A.; Zhu, Q. H., Formation and Photodissociation of Transition Metal-Sulfur Binary Cluster Ions. *J. Chin. Chem. Soc.* **1995,** 42, (2), 455-460.

9. Fisher, K.; Dance, I.; Willett, G., Lanthanide-sulfur gas-phase chemistry: reactions of Ln(+) with S-8. *Journal of the Chemical Society-Dalton Transactions* **1998**, (6), 975-980.

10. Chen, H.; Huang, R. B.; Lu, X.; Tang, Z. C.; Xu, X.; Zheng, L. S., Studies on carbon/sulfur cluster anions produced by laser vaporization: Experiment (collision-induced dissociation) and theory (ab initio calculation). I. $C_2S_m^-$ (1 <= m <= 11). *J. Chem. Phys.* **2000,** 112, (21), 9310-9318.

11. Liu, Z. Y.; Wang, C. R.; Huang, R. B.; Zheng, L. S., Mass Distributions of Binary Aluminum Cluster Anions Al(N)X(M)(-) (X=O, S, P, as, C). *Int. J. Mass Spectrom. Ion Processes* **1995,** 141, (3), 201-208.

12. Nakajima, A.; Zhang, N.; Kawamata, H.; Hayase, T.; Nakao, K.; Kaya, K., Photoelectron-Spectroscopy and Mass Distributions of Aluminum-Sulfur Cluster Anions ($Al_nS_m^-$). *Chem. Phys. Lett.* **1995,** 241, (4), 295-300.

13. Zhang, N.; Shi, Y.; Gao, Z.; Kong, F. N.; Zhu, Q. H., Aluminum-Sulfur Cluster Ions - Formation and Photolysis. *J. Chem. Phys.* **1994,** 101, (2), 1219-1224.

14. Hill, C. L.; Prossermccartha, C. M., Homogeneous Catalysis by Transition-Metal Oxygen Anion Clusters. *Coord. Chem. Rev.* **1995,** 143, 407-455.

15. Aiken, J. D.; Lin, Y.; Finke, R. G., A perspective on nanocluster catalysis: Polyoxoanion and (n-$C_4H_9N^+$ stabilized Ir(O) (similar to 300) nanocluster 'soluble heterogeneous catalysts'. *Journal of Molecular Catalysis a-Chemical* **1996,** 114, (1-3), 29-51.

16. Libuda, J.; Schalow, T.; Brandt, B.; Laurin, M.; Schauermann, S., Model studies in heterogeneous catalysis at the microscopic level: from the structure and composition of surfaces to reaction kinetics. *Microchimica Acta* **2006,** 156, (1-2), 9-20.

17. Ayers, T. M.; Fye, J. L.; Li, Q.; Duncan, M. A., Synthesis and isolation of titanium metal cluster complexes and ligand-coated nanoparticles with a laser vaporization flowtube reactor. *J. Cluster Sci.* **2003,** 14, (2), 97-113.

18. France, M. R.; Buchanan, J. W.; Robinson, J. C.; Pullins, S. H.; Tucker, J. L.; King, R. B.; Duncan, M. A., Antimony and bismuth oxide clusters: Growth and decomposition of new magic number clusters. *J. Phys. Chem. A* **1997,** 101, (35), 6214-6221.

19. van Heijnsbergen, D.; Demyk, K.; Duncan, M. A.; Meijer, G.; von Helden, G., Structure determination of gas phase aluminum oxide clusters. *Phys. Chem. Chem. Phys.* **2003,** 5, (12), 2515-2519.

20. van Heijnsbergen, D.; von Helden, G.; Meijer, G.; Duncan, M. A., Infrared resonance-enhanced multiphoton ionization spectroscopy of magnesium oxide clusters. *J. Chem. Phys.* **2002,** 116, (6), 2400-2406.

21. *Clusters of Atoms and Molecules II*. Springer-Verlag: Berlin, 1994; Vol. 56.

22. *Clusters of Atoms and Molecules I*. 2nd ed.; Springer-Verlag: Berlin, 1995; Vol. 52.

23. Bach, S. B. H.; Mcelvany, S. W., Determination of the Ionization-Potentials of Aluminum-Oxides Via Charge-Transfer. *J. Phys. Chem.* **1991,** 95, (23), 9091-9094.

24. Martinez, A.; Tenorio, F. J.; Ortiz, J. V., Electronic structure of Al_3O_n and $Al_3O_n^-$ (n=1-3) clusters. *J. Phys. Chem. A* **2001,** 105, (38), 8787-8793.

25. von Helden, G.; Kirilyuk, A.; van Heijnsbergen, D.; Sartakov, B.; Duncan, M. A.; Meijer, G., Infrared spectroscopy of gas-phase zirconium oxide clusters. *Chem. Phys.* **2000,** 262, (1), 31-39.

26. von Helden, G.; van Heijnsbergen, D.; Meijer, G., Resonant ionization using IR light: A new tool to study the spectroscopy and dynamics of gas-phase molecules and clusters. *J. Phys. Chem. A* **2003,** 107, (11), 1671-1688.

27. Deshpande, M.; Kanhere, D. G.; Pandey, R., Structural and electronic properties of neutral and ionic Ga_nO_n clusters with n=4-7. *J. Phys. Chem. A* **2006,** 110, (10), 3812-3813.

28. Gowtham, S.; Costales, A.; Pandey, R., Theoretical study of neutral and ionic states of small clusters of Ga_mO_n (m, n = 1, 2). *J. Phys. Chem. B* **2004,** 108, (45), 17295-17300.

29. Gowtham, S.; Deshpande, M.; Costales, A.; Pandey, R., Structural, energetic, electronic, bonding, and vibrational properties of Ga_3O, Ga_3O_2, Ga_3O_3, Ga_2O_3, and GaO_3 clusters. *J. Phys. Chem. B* **2005,** 109, (31), 14836-14844.

30. He, H. Y.; Orlando, R.; Blanco, M. A.; Pandey, R.; Amzallag, E.; Baraille, I.; Rerat, M., First-principles study of the structural, electronic, and optical properties of Ga_2O_3 in its monoclinic and hexagonal phases. *Phys. Rev. B* **2006,** 74, (19).

31. King, F. L.; Dunlap, B. I.; Parent, D. C., Characterization of Cluster Ions Produced by the Sputtering or Direct Laser Vaporization of Group-13 Metal (Al, Ga, and In) Oxides. *J. Chem. Phys.* **1991,** 94, (4), 2578-2587.

32. Tanaka, I.; Mizuno, M.; Adachi, H., Electronic structure of indium oxide using cluster calculations. *Phys. Rev. B* **1997,** 56, (7), 3536-3539.

33. Tomita, T.; Yamashita, K.; Hayafuji, Y.; Adachi, H., The origin of n-type conductivity in undoped In_2O_3. *Appl. Phys. Lett.* **2005,** 87, (5), -.

34. Seo, D. K.; Corbett, J. D., Perspectives: Chemistry - Aromatic metal clusters. *Science* **2001,** 291, (5505), 841-842.

35. Cotton, F. A.; Wilkinson, G.; Murillo, C.; Bochmann, M., *Advanced Inorganic Chemistry, 6th ed.* John Wiley & Sons, Inc.: New York, 1999.

36. Muetterties, E. L.; Knoth, W. H., *Polyhedral Boranes*. Dekker: New York, 1968; p 197.

37. Wade, K., Structural and bonding patterns in cluster chemistry. *Advances in Inorganic Chemistry and Radiochemistry* **1976,** 18, 1-66.

38. Grimes, R. N., *Carboranes*. Academic: New York, 1970; p 272.

39. Muetterties, E. L. R., T. N.; Band, Elliot; Brucker, C. F.; Pretzer, W. R, Clusters and surfaces. *Chem. Rev.* **1979,** 79, 91-137.

40. Wheeler, R. G.; Laihing, K.; Wilson, W. L.; Allen, J. D.; King, R. B.; Duncan, M. A., Neutral Gas-Phase Analogs of Condensed-Phase Post-Transition-Metal Cluster Ions - Laser Vaporization and Photoionization of Sn/Bi and Pb/Sb Alloys. *J. Am. Chem. Soc.* **1986,** 108, (25), 8101-8102.

41. Wheeler, R. G.; Laihing, K.; Wilson, W. L.; Duncan, M. A., Growth-Patterns in Binary Clusters of Group-IV and Group-V Metals. *J. Chem. Phys.* **1988,** 88, (4), 2831-2839.

42. King, R. B., Chemical Bonding Topology of Bare Post-Transition-Metal Clusters - Analogies between Condensed-Phase and Gas-Phase Species. *J. Phys. Chem.* **1988,** 92, (15), 4452-4456.

43. Zintl, E., Intermetallic compounds. *Angew. Chem.* **1939,** 52, 1-6.

44. Belin, C.; Tillard-Charbonnel, M., Aspects of anionic framework formation. Clustering of p-block elements. *Coord. Chem. Rev.* **1998,** 178, 178-180.

45. Corbett, J. D., Diverse naked clusters of the heavy main-group elements. Electronic regularities and analogies. *Structural and Electronic Paradigms in Cluster Chemistry* **1997,** 87, 157-193.

46. Axe, F. U.; Marynick, D. S., Relationships between Bonding and Structure in Tetranuclear Heteroatomic Zintl Anions Containing 20 Valence-Electrons. *Inorg. Chem.* **1988,** 27, (8), 1426-1431.

47. Dong, Z.-C.; Corbett, J. D., A8Tl11 (A = K, Rb, or Cs) phases with hypoelectronic Tl117- cluster anions: syntheses, structure, bonding, and properties. *J. Cluster Sc.* **1995,** 6, (1), 187-201.

48. Van der Lugt, W., Zintl ions as structural units in liquid alloys. *Physica Scripta* **1991,** T39, 372.

49. Xu, L.; Sevov, S. C., Heteroatomic deltahedral clusters of main-group elements: Synthesis and structure of the Zintl ions $[In_4Bi_5](3-)$, $[InBi_3](2-)$, and $[GaBi_3](2-)$. *Inorg. Chem.* **2000,** 39, (23), 5383-5389.

50. Knight, W. D.; Deheer, W. A.; Clemenger, K.; Saunders, W. A., Electronic Shell Structure in Potassium Clusters. *Solid State Commun.* **1985,** 53, (5), 445-446.

51. Knight, W. D.; Clemenger, K.; Deheer, W. A.; Saunders, W. A.; Chou, M. Y.; Cohen, M. L., Electronic Shell Structure and Abundances of Sodium Clusters. *Phys. Rev. Lett.* **1984,** 52, (24), 2141-2143.

52. Bergeron, D. E.; Castleman, A. W.; Morisato, T.; Khanna, S. N., Formation of $Al_{13}I^-$: Evidence for the superhalogen character of Al_{13}^-. *Science* **2004,** 304, (5667), 84-87.

53. Bergeron, D. E.; Roach, P. J.; Castleman, A. W.; Jones, N.; Khanna, S. N., Al cluster superatoms as halogens in polyhalides and as alkaline earths in iodide salts. *Science* **2005,** 307, (5707), 231-235.

54. Pellarin, M.; Lerme, J.; Baguenard, B.; Broyer, M.; Vialle, J. L., Shell Structure in Photoionization Spectra of Trivalent Metal-Clusters. *Berichte Der Bunsen-Gesellschaft-Physical Chemistry Chemical Physics* **1992,** 96, (9), 1212-1215.

55. Persson, J. L.; Whetten, R. L.; Cheng, H. P.; Berry, R. S., Evidence for Quantized Electronic Level Structure for 100-1300 Electrons in Metal-Atomic Clusters. *Chem. Phys. Lett.* **1991,** 186, (2-3), 215-222.

56. Schriver, K. E.; Persson, J. L.; Honea, E. C.; Whetten, R. L., Electronic Shell Structure of Group-IIIa Metal Atomic Clusters. *Phys. Rev. Lett.* **1990,** 64, (21), 2539-2542.

57. Lerme, J.; Bordas, C.; Pellarin, M.; Baguenard, B.; Vialle, J. L.; Broyer, M., Semiclassical Analysis of the Electronic Shell Structure in Metal-Clusters. *Phys. Rev. B* **1993,** 48, (12), 9028-9044.

58. Brack, M., The Physics of Simple Metal-Clusters - Self-Consistent Jellium Model and Semiclassical Approaches. *Rev. Mod. Phys.* **1993,** 65, (3), 677-732.

59. Deheer, W. A., The Physics of Simple Metal-Clusters - Experimental Aspects and Simple-Models. *Rev. Mod. Phys.* **1993,** 65, (3), 611-676.

60. Cottancin, E.; Pellarin, M.; Lerme, J.; Palpant, B.; Baguenard, B.; Vialle, J. L.; Broyer, M., Unimolecular dissociation of trivalent metal cluster ions (Al_n^+, Ga_n^+, $In_n^{+)}$: Evidence for a transition from covalent to metallic bonding. *Zeitschrift Fur Physik D-Atoms Molecules and Clusters* **1997,** 40, (1-4), 288-293.

61. Cornett, D. S.; Peschke, M.; Laihing, K.; Cheng, P. Y.; Willey, K. F.; Duncan, M. A., Reflectron Time-of-Flight Mass-Spectrometer for Laser Photodissociation. *Rev. of Sc. Instr.* **1992,** 63, (4), 2177-2186.

62. Cornett, D. S.; Amster, I. J.; Duncan, M. A.; Rao, A. M.; Eklund, P. C., Laser Desorption Mass-Spectrometry of Photopolymerized C-60 Films. *J. Phys. Chem.* **1993,** 97, (19), 5036-5039.

63. Hearley, A. K.; Johnson, B. F. G.; McIndoe, J. S.; Tuck, D. G., Mass spectrometric identification of singly-charged anionic and cationic sulfur, selenium, tellurium and phosphorus species produced by laser ablation. *Inorg. Chim. Acta* **2002,** 334, 105-112.

64. Steudel, R.; Holz, B., Detection of Reactive Sulfur Molecules (S_6, S_7, S_9, S-Infinity) in Commercial Sulfur, in Sulfur Minerals, and in Sulfur Melts Slowly Cooled to 20-Degrees-C. *Zeitschrift Fur Naturforschung Section B-a Journal of Chemical Sciences* **1988,** 43, (5), 581-589.

65. Steudel, R.; Eckert, B., Solid sulfur allotropes. *Elemental Sulfur and Sulfur-Rich Compounds I* **2003,** 230, 1-79.

66. Knight, L. B.; Kirk, T. J.; Herlong, J.; Kaup, J. G.; Davidson, E. R., Electron spin resonance matrix isolation studies of (AlO)-Al-27-O-16,17, (GaO)-Ga-69,71-O-16,17 and (InO)-In-115-O-16,17: Observed hyperfine interactions compared with ab initio theoretical results. *J. Chem. Phys.* **1997,** 107, (18), 7011-7019.

67. Molek, K. S.; Jaeger, T. D.; Duncan, M. A., Photodissociation of vanadium, niobium, and tantalum oxide cluster cations. *J. Chem. Phys.* **2005,** 123, (14).

68. Janssens, E.; Neukermans, S.; Vanhoutte, F.; Silverans, R. E.; Lievens, P.; Navarro-Vazquez, A.; Schleyer, P. V., Ionization potentials and structures of small indium monoxide clusters. *J. Chem. Phys.* **2003,** 118, (13), 5862-5871.

Table 3.1. Possible mass assignments for peaks in the aluminum sulfur spectra.

Mass	Possible $Al_nS_m^+$ Assignments
27	(1,0)
65	(0,2)
119	(2,2)
124	(1,3)
127	(0,4)
152	(2,3)
156	(1,4)
160	(0,5)
164	(6,0)*
184	(2,4)
189	(7,0)* (1,5)
192	(0,6)
215	(2,5)
221	(7,1) (1,6) (0,7)
192	(6,1) (0.7)
215	(2,5) (8,0)
221	(7,1) (1,6) (0,7)
225	(6,2) (0,7)
248	(8,1) (2,6) (1,7)
254	(1,7) (0,8)
258	(6,3) (0,8)

276	(9,1) (3,5) (2,7)
281	(8,2) (2,7) (1,8)
286	(1,8) (0,9)
292	(6,4) (5,5)
309	(9,2)* (2,8)
314	(8,3) (9,2)
318	(0,10)*
341	(2,9)
352	(13,0)* (6,6) (0,11)*
369	(9,4) (3,9)
401	(10,4) (9,5) (3,10)
462	(4,11) (3,12)
506	(8,9) (1,15)*
522	(11,7) (5,12) (4,13) (3,14)
599	(8,12) (2,17)*
616	(11,10) (10,11) (5,15)
643	(12,10) (11,11) (6,15)
659	(9,13) (8,14) (3,18) (2,19)*
676	(13,10) (12,11) (7,15) (6,16)

*These peaks are improbable when compared with the pure element spectra. Clusters of this many elements of this atom are not observed

Table 3.2. The distribution of stoichiometries for prominent metal sulfur cations that satisfy Wade's rules stoichiometries.

$Al_nS_m^+$	#p electrons	# total electrons	Wade's rules
1,3	12	14	nido
1,4	16	18	arachno
$Ga_nS_m^+$			
5,4	20	30	closo
$In_nS_m^+$			
5,4	20	30	closo
7,5	26	40	closo
7,6	30	44	nido
9,7	36	54	nido
9,8	40	58	arachno

FIGURES

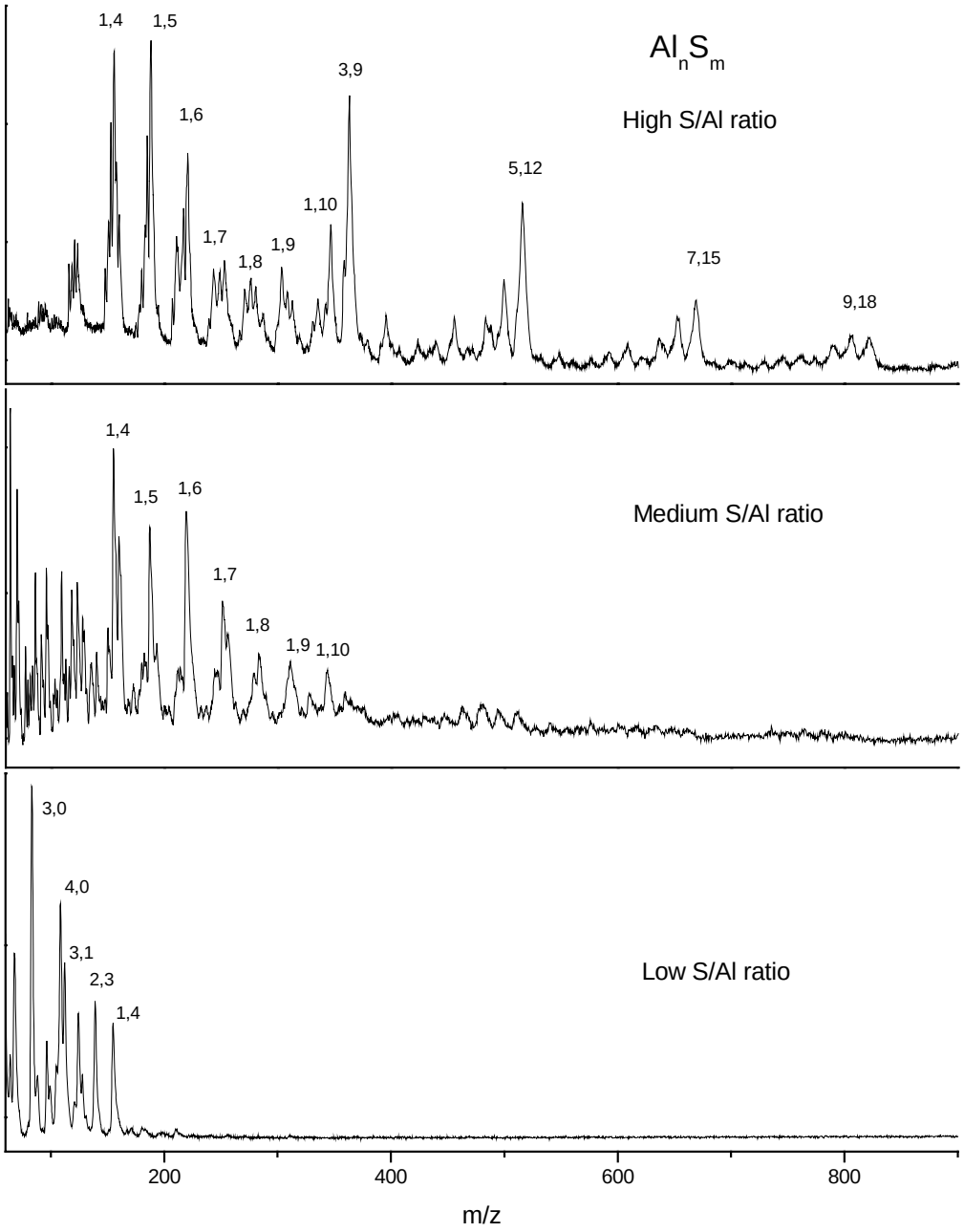

Figure 3.1. Time-of-flight mass spectrum obtained for mixtures of aluminum and sulfur ablated with 532 nm light. All peaks including smaller ones are assigned to mixed aluminum sulfur cluster species with varying combinations.

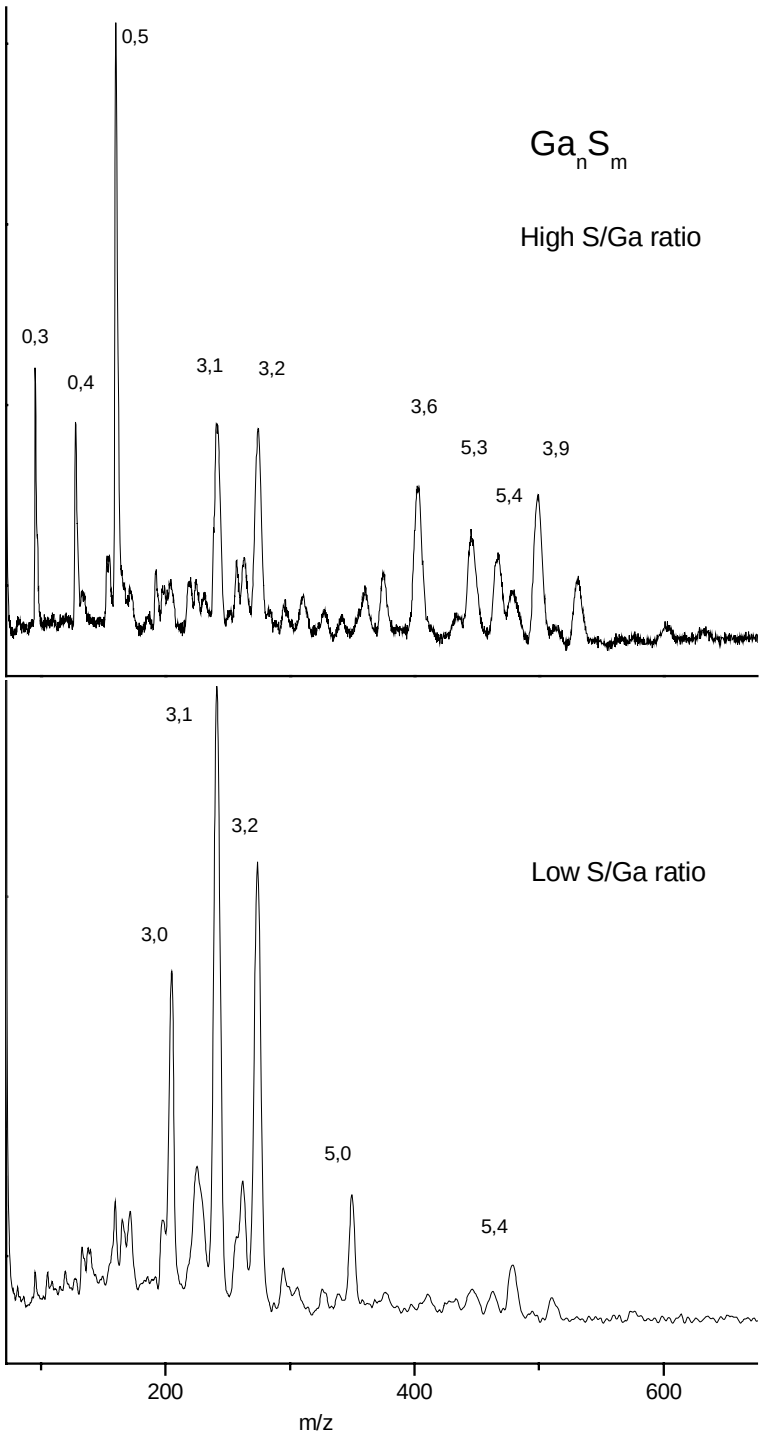

Figure 3.2. Time-of-flight mass spectrum obtained for different mixtures of gallium and sulfur ablated with 532 nm light.

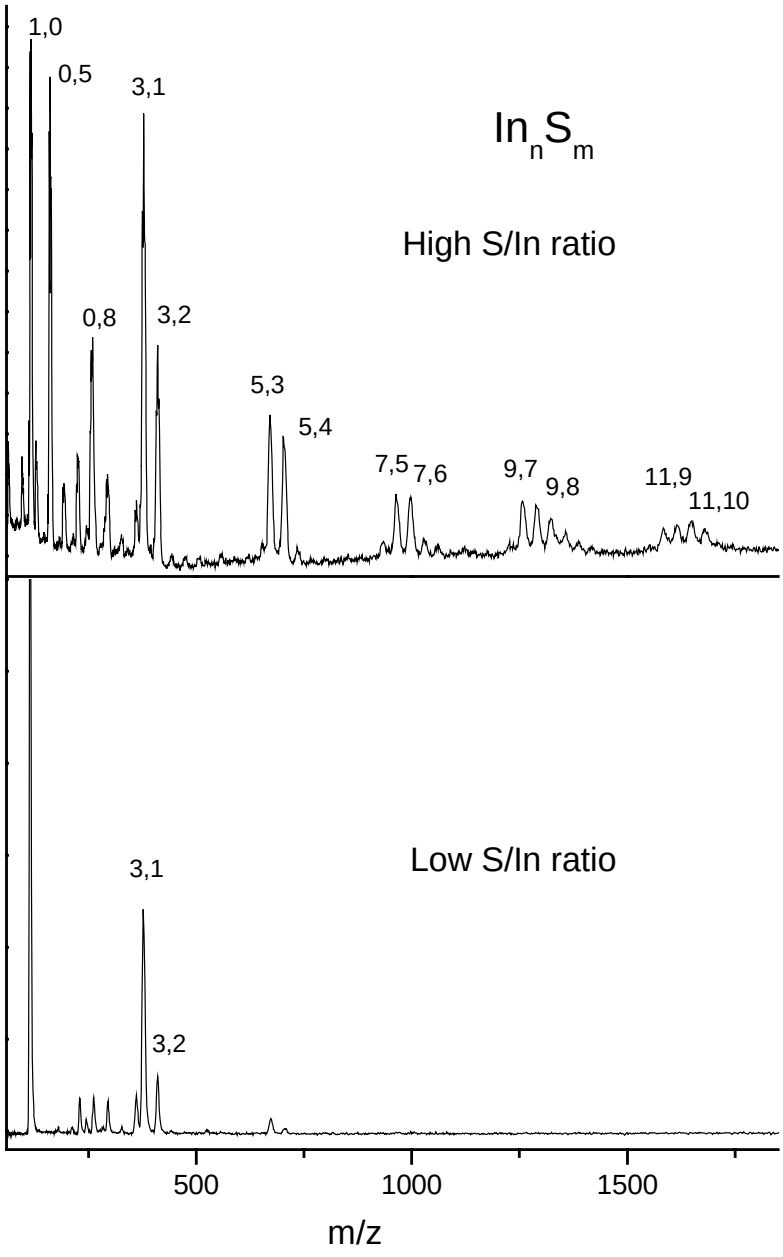

Figure 3.3. Time-of-flight mass spectrum obtained for mixtures of indium and sulfur ablated with 532 nm light.

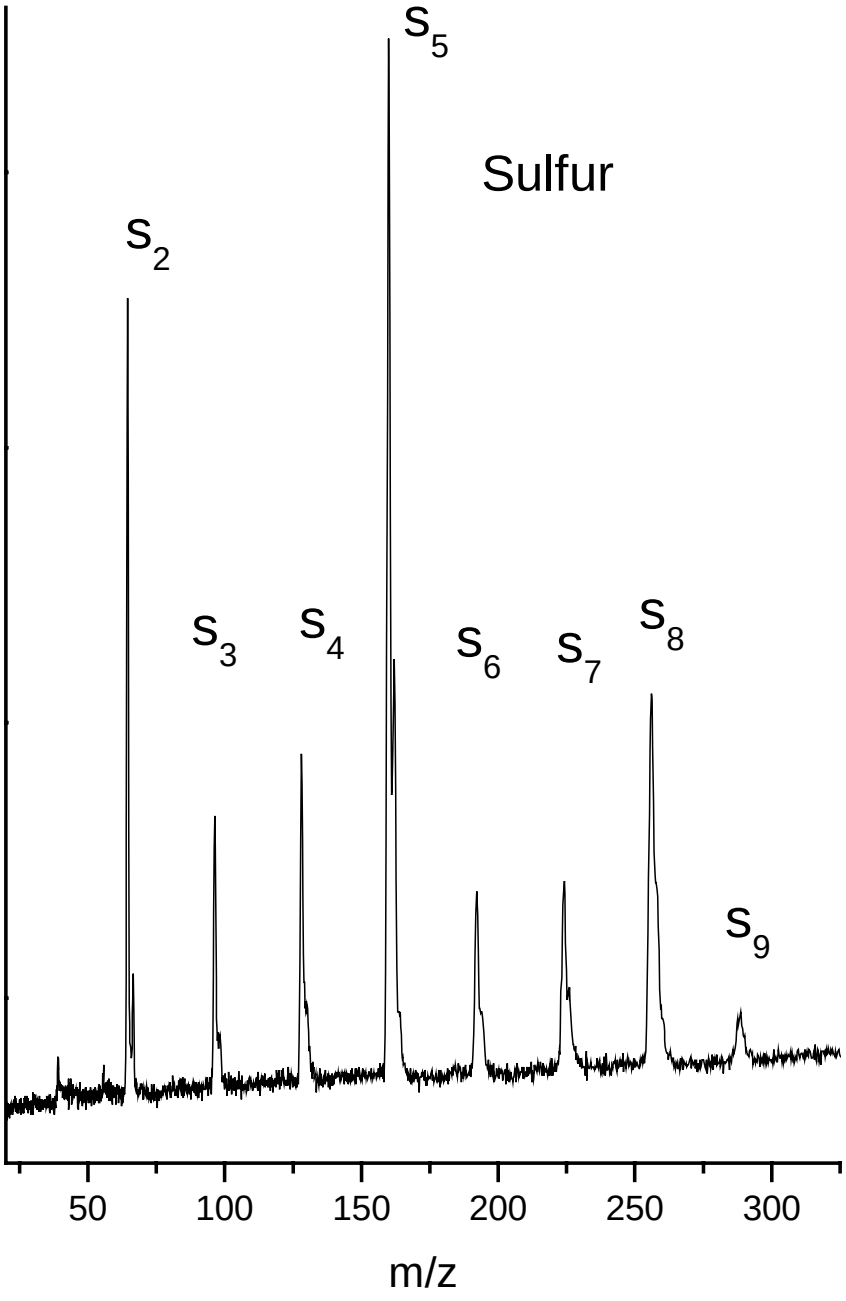

Figure 3.4. Time-of-flight mass spectrum for sulfur ablated with 532 nm light.

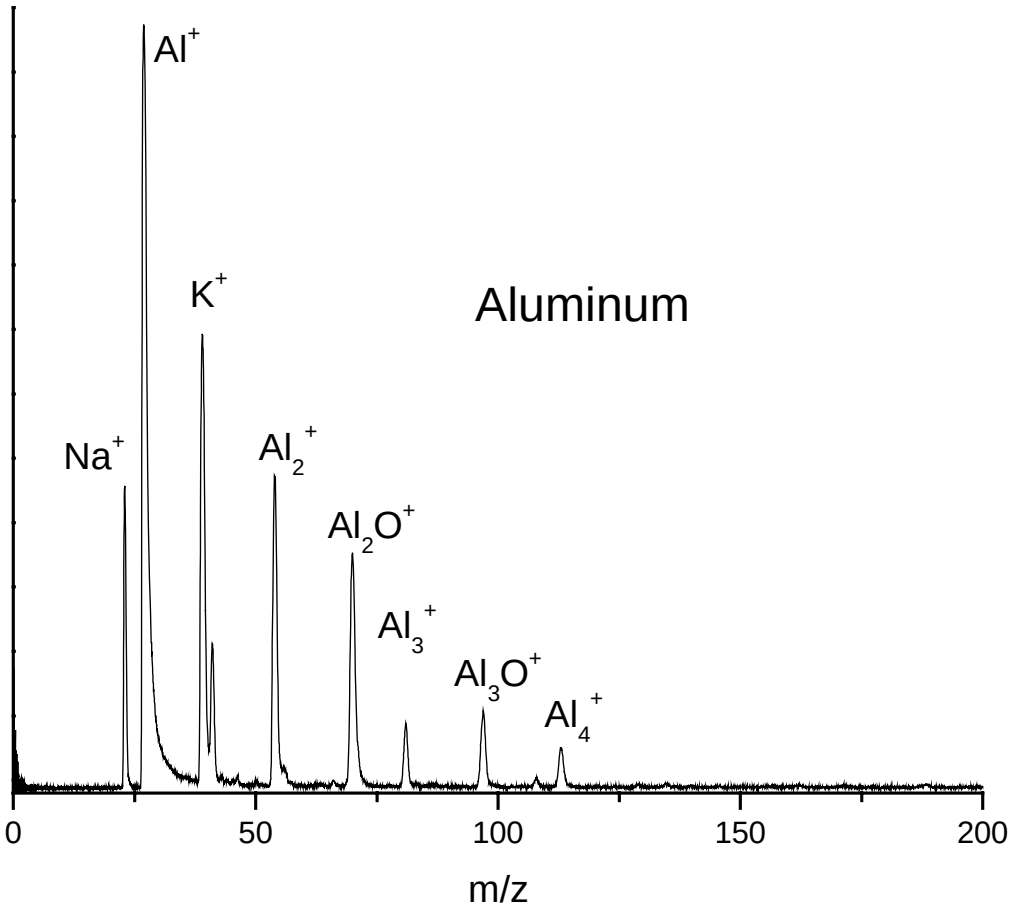

Figure 3.5. A time-of-flight mass spectrum of aluminum and aluminum oxide clusters.

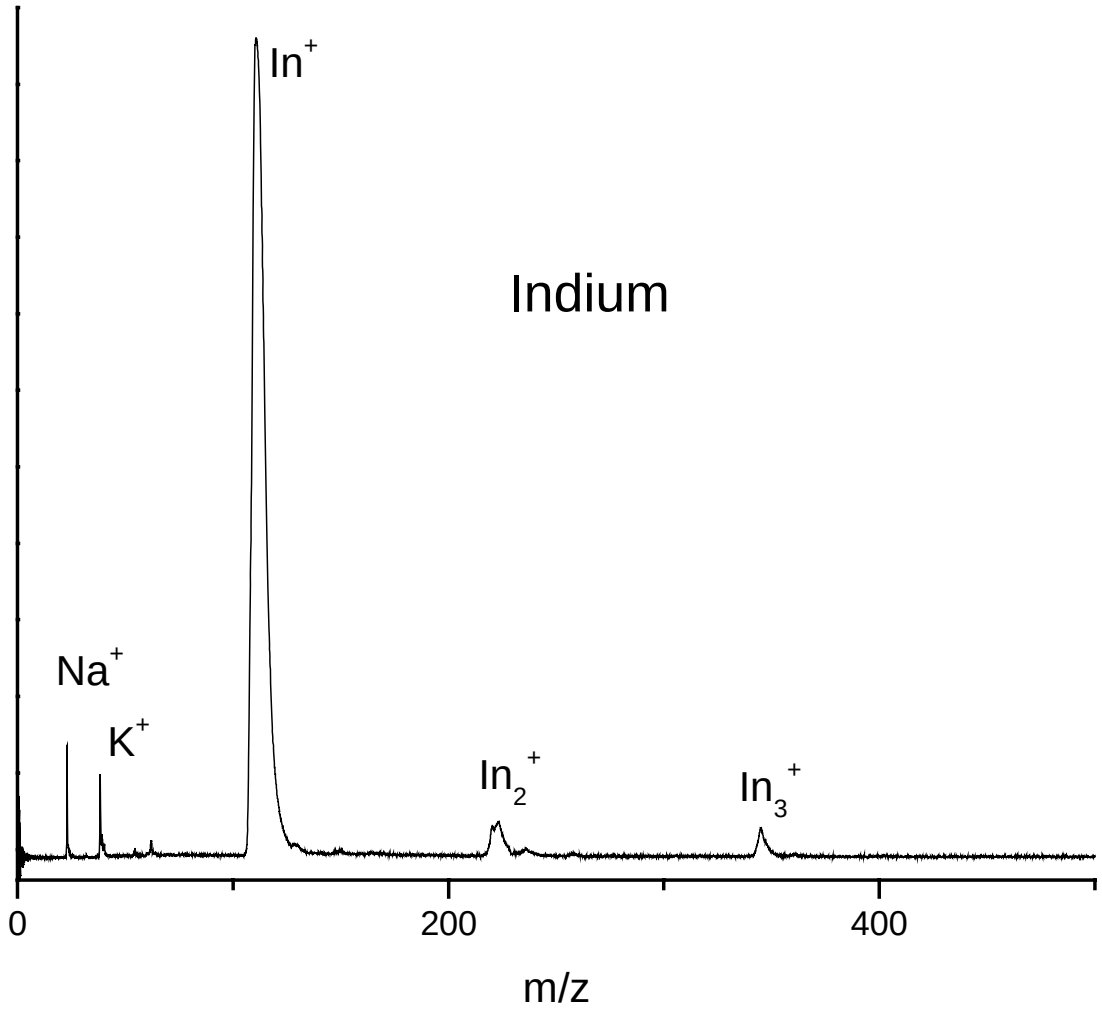

Figure 3.6. A time-of-flight mass spectrum of indium clusters.

CHAPTER 4

CARBON ONIONS[1]

1. Ham, P.B.; Ayers, T.M.; Duncan, M.A. To be submitted to International Journal of Mass Spectrometry.

4.1 BACKGROUND

During an intense workweek in the 1980's, Curl, Kroto, Smalley, and coworkers discovered a new allotrope of carbon, buckminster fullerene, in a molecular beam by laser vaporization of a graphite target.[1-4] They speculated that it consisted of 60 carbon atoms in an icosahedral structure, the shape of a soccer ball as in Figure 4.1. This news was received with great enthusiasm because it was the first time in the 20th century that a new allotrope of any element had been discovered.[5] Because it was discovered in the gas phase, it remained a curiosity until it was produced in the condensed phase by Kratschmer and Huffman using resistively heated carbon rods in a helium atmosphere.[6] Their method, using an arc discharge in 200 torr helium, has become an efficient way to produce C_{60} in gram quantities.[2, 7] It became readily available, which provided a huge stimulus to the field. Experiments soon proved that C_{60} could have endohedral metal atoms[8] that alter its physical properties so that it is superconductive at high temperatures.[9] C_{60}'s many interesting properties also sparked enthusiastic investigations for new allotropes of carbon.

In 1992, Iijima and coworkers discovered that carbon can exist in tubular forms, now known as carbon nanotubes.[2, 10] They can be produced via an arc discharge in liquid nitrogen,[11] in the gas phase (1 nm diameter single walled carbon nanotubes),[12] by condensation of a laser-vaporized carbon-nickel-cobalt mixture,[13] and by the catalytic chemical vapor deposition of methane.[14] Nanotubes are extremely interesting because they have the largest known Young's modulus and tensile strength.[2] In theory, they will have tunable mechanical, electrical, and magnetic properties based on their diameter.[2, 12, 15]

Later, a fifth allotrope of carbon was discovered by Ugarte and coworkers in 1992.[16] They called this form a carbon nano-onion because of its unique structure. It consists of several

spherical balls of carbon nested inside each other like Russian dolls. At its core is a C_{60} molecule, and larger spheres such as C_{240} and C_{540} compose its outer layers. They form because small graphene sheets have dangling bonds on their edges. Therefore, the sheets bend to stabilize their unbound edges. This results in the formation of large multishelled fullerenes. Carbon onions can be produced by electron beam irradiation of amorphous carbon in a transmission electron microscope[16-18]; by the annealing of nanodiamonds at 1500-1700ºC[19]; implantation of 120 keV carbon ions into silver resulting in the precipitation of carbon onions[20]; by radio-frequency plasma-enhanced chemical vapor deposition[21]; and by using an arc between graphitic electrodes in water.[22] Sano and coworkers found that although the density of carbon onions is greater than water, the particles float! They suggested that the carbon onion particles float because of their hydrophobicity.[22] However, Rettenbacher and coworkers found that carbon onions were also present in the bottom of the water container.

Annealing of nanodiamonds and an arc discharge in water are currently the two primary means of producing carbon onions. These methods produce different size carbon onions with different properties. Annealed-nanodiamond carbon onions are typically smaller than carbon onions produced by an arc discharge.[23] They are typically 5-6 nm in diameter and have 6-8 shells.[23] Carbon onions produced in an arc discharge are usually larger. They typically have more than 20 shells and are more than 14-22 nm in diameter.[23] The carbon onions produced from the annealing of nanodiamonds are less uniform than those from the arc method as illustrated by the Raman spectra.[23] Graphite has a single sharp peak at 1,575 cm^{-1} that is due to the vibrations of its sp^2 hybridized carbons. This peak is present in the Raman spectra of carbon onions as well and is called the G band. Other carbon materials have a peak at about 1307 cm^{-1}. This is called the D band, and it is due to the vibrations of sp^3 hybridized carbons. Since sp^3

carbons are considered defects in the carbon onion, the D band represents the lack of uniformity of the carbon onion. The D/G band ratio is used to compare defects between different carbon onions. In this case, carbon onions produced from nanodiamonds were less uniform. However, Ugarte found that carbon onions that were formed by the arc method and subsequently annealed had the sharpest Raman peaks.[23-25] X-Ray diffraction data suggested that carbon onions from nanodiamonds have more uniform spacing between most layers but that they may have more dangling ends, as evidenced by the larger spacing to the right of the main peak.[23] In the X-Ray spectrum, the 0.334 nm spacing between layers is comparable to graphite.[23] An electron spin resonance (ESR) spectrum demonstrated that carbon onions from nanodiamonds have unpaired electrons, which suggests that the carbon onions from nanodiamonds may have more bonding defects.[23, 25] This corroborates the dangling bond hypothesis from the X-Ray spectrum. Therefore, these data suggest that nanodiamond carbon onions are smaller, have more uniform spacing between layers, and have more dangling bonds than carbon onions produced by arcing.

While much work has been done on carbon onions, no mass spectrometry measurements have been made. The only size verification experiments that have been done so far are electron microscopy. These cannot accurately verify the sizes or their distribution. Mass measurements could confirm the size of these particles; however, carbon onions pose a significant problem to mass spectrometry because the particles are so large. Carbon onions produced by arcing would be more than 80,000 amu. A typical quadrupole mass spectrometer can only measure up to 800 amu. However, time of flight mass spectrometers (TOFMS) can measure to more than 800,000 amu. Therefore, it is possible that TOFMS can be used to determine the size of carbon onions.

4.2 EXPERIMENTAL

The laser desorption time-of-flight mass spectrometer used in these experiments has been described previously.[26] It is a Bruker Autoflex mass spectrometer with the capability for high acceleration fields (up to 30 kV) and delayed pulsed extraction for improved resolution.[27] Carbon onion powders produced by the annealing of nanodiamonds or a graphite arc in water were obtained from Amit Palkar and Frederic Melin of Louis Echegoyen's group at Clemson University. Some powders had been previously treated with a mixture of nitric and sulfuric acid in equal concentration in order to "peel" the onions by Palkar and Melin.[23] The carbon onion powders are pressed onto a stainless steel block. Smooth sample surfaces are essential to obtain the best results in these laser desorption experiments. Once prepared, the samples are inserted into the mass spectrometer for analysis. All chemicals are used as received without further purification.

Desorption and ionization are accomplished by focusing a nitrogen laser onto the sample inside the mass spectrometer. The fluence of the laser is adjusted to minimize fragmentation of the carbon onions; energies of 20-50 μJ/pulse are employed for these experiments. Once the material is desorbed, cations are accelerated down the flight tube at an energy of 20 keV and focused with an einzel lens before reaching the detector. Mass spectra are collected, averaged, and transferred to a PC for processing.

4.3 RESULTS

Mass spectra were obtained for carbon onions produced in an arc source before treatment with concentrated acid and after treatment. Figure 4.2 depicts the mass spectra of "unpeeled" and "peeled" carbon onions. The spectra have similar shapes and there are no magic numbers. Rather, there is essentially a lognormal distribution of masses from about 10,000 amu to 350,000 amu. However, the major difference is that the peeled curve is shifted to lower mass. The

maximum in the unpeeled mass distribution occurs at about 115,500 amu while the maximum in the peeled peak distribution occurs at about 98,400 amu. Therefore, there is a difference of about 17,100 amu between the maximum peaks. To determine the number of layers in the carbon onion based on the mass, the number of atoms per layer must be known. The number of atoms in a layer can be calculated from $N=60b^2$ where b is the layer number and N is the number of atoms.[28] Then, the number of atoms in all of the layers can be added and multiplied by the mass of carbon to get the total mass of the number of layers. The masses of carbon onions from one layer to 30 layers are tabulated in Table 4.1. According to the table, the maximum peaks of the carbon onions from the spectra are from carbon onions with about seven layers, corresponding to a mass of 100,800 amu. The range of masses yields a range of layers from three layers (10,080 amu) to 11 layers (364,320 amu).

4.4 DISCUSSION

According to Table 4.1, if carbon onions produced in an arc source have 20-30 layers, then they should primarily have masses ranging from 2,066,400 amu to 6,807,600 amu. However, the masses ranged from 10,080 amu to 364,320 amu. This implies that the number of layers is much less than expected and that carbon onions formed in an arc source may be, on average, smaller than previously thought. Current knowledge about the size of carbon onions is primarily based on electron microscopy. However, electron microscopy can have a significant amount of sampling bias because only a small portion of the sample is seen, the viewed portion may not represent the entire sample, and most importantly, bigger objects are easier to see. According to the mass spectra, carbon onions produced in an arc source are smaller than anticipated. However, another interpretation is that TOFMS does not sample larger onions

effectively. Larger carbon onions may not desorb as well or ionize as well. The laser could also be fragmenting the onions.

According to Table 4.1, if a carbon onion has seven layers and loses a layer, its mass should decrease from 100,800 amu to 65,520 amu, a difference of 35,280 amu. This mass corresponds to 2,940 carbon atoms. However, the difference in mass between the original seven-layered sample and the sample that was treated with concentrated acid to remove a layer was 17,100 amu. This mass represents about 1,425 atoms. This implies that while the acid treatment was successful in removing about half of a layer, it was not successful in removing an entire layer.

Since there is one large, broad peak with no magic numbers in the mass spectra, it appears that plus or minus several carbon atoms does not make a large impact on the stability of the carbon onion. Also, the maximum peak mass lies between the mass for two layers. This implies that the onions may not have an exact shape of many concentric spheres nested inside each other. Rather, some layers may be more like ellipsoids that have a larger distance between the other layers in some areas because they may have other impurities inside. They may have interstitial atoms such as metals or even graphitic layers that could alter the mass of the onion as well as the distance between layers and the number of atoms in a layer. Mechanisms have even been proposed concerning the manner in which deformations occur and how the number of atoms in a layer changes based on the deformations.[29] The X-ray diffraction data supports the idea that the distance between layers may be greater due to ellipsoid shapes or interstitial atoms as there is a signal 1/4 of the intensity of the graphite 0.334 nm peak for d-spacings greater than 0.334 nm.[23] Another potential cause of the large lognormal distribution of masses is that the outside layers of carbon onions may not necessarily be complete. This is the most likely

explanation for the discrepancies; since only half a layer was removed in the acid treatment, only half a layer may have been present in the first place. With larger onions, this is possible because the outer layers become more and more like planar graphite, with less five membered rings for curvature and more six membered rings. Even in the electron micrographs, some of the onions do not appear complete, perfectly spherical, or without defects.[23]

4.5 CONCLUSIONS

Carbon onions produced in an arc source and analyzed using mass spectrometry appear to have the same number of layers as carbon onions produced from nanodiamonds. The layers of these carbon onions are not perfect and have defects. Portions of the layers can be removed using a treatment with concentrated nitric acid. This suggests that with multiple treatments of acid, potentially more layers of the carbon onion could be removed. However, these experiments have not yet been done. Therefore, more investigations are necessary to verify the effects of multiple acid treatments on these interesting nanoparticles.

4.6 REFERENCES

1. Kroto, H. W.; Heath, J. R.; Obrien, S. C.; Curl, R. F.; Smalley, R. E., C-60 - Buckminsterfullerene. *Nature* **1985,** 318, (6042), 162-163.

2. Dresselhaus, M. S.; Dresselhaus, G.; Eklund, P., *Science of Fullerenes and Carbon Nanotubes*. Academic Press, Inc.: San Diego, 1996; p 965.

3. Kroto, H., Space, Stars, C-60, and Soot. *Science* **1988,** 242, (4882), 1139-1145.

4. Curl, R. F.; Smalley, R. E., Probing C-60. *Science* **1988,** 242, (4881), 1017-1022.

5. Subramoney, S., Novel nanocarbons - Structure, properties, and potential applications. *Advanced Materials* **1998,** 10, (15), 1157.

6. Kratschmer, W.; Lamb, L. D.; Fostiropoulos, K.; Huffman, D. R., Solid C-60 - a New Form of Carbon. *Nature* **1990,** 347, (6291), 354-358.

7. Haufler, R. E.; Conceicao, J.; Chibante, L. P. F.; Chai, Y.; Byrne, N. E.; Flanagan, S.; Haley, M. M.; Obrien, S. C.; Pan, C.; Xiao, Z.; Billups, W. E.; Ciufolini, M. A.; Hauge, R. H.; Margrave, J. L.; Wilson, L. J.; Curl, R. F.; Smalley, R. E., Efficient Production of C_{60} (Buckminsterfullerene), $C_{60}H_{36}$, and the Solvated Buckide Ion. *J. Phys. Chem.* **1990,** 94, (24), 8634-8636.

8. Haddon, R. C.; Hebard, A. F.; Rosseinsky, M. J.; Murphy, D. W.; Duclos, S. J.; Lyons, K. B.; Miller, B.; Rosamilia, J. M.; Fleming, R. M.; Kortan, A. R.; Glarum, S. H.; Makhija, A. V.; Muller, A. J.; Eick, R. H.; Zahurak, S. M.; Tycko, R.; Dabbagh, G.; Thiel, F. A., Conducting Films of C_{60} and C_{70} by Alkali-Metal Doping. *Nature* **1991,** 350, (6316), 320-322.

9. Hebard, A. F., Superconductivity in Doped Fullerenes. *Physics Today* **1992,** 45, (11), 26-32.

10. Iijima, S., Helical Microtubules of Graphitic Carbon. *Nature* **1991,** 354, (6348), 56-58.

11. Ishigami, M.; Cumings, J.; Zettl, A.; Chen, S., A simple method for the continuous production of carbon nanotubes. *Chem Phys Lett* **2000,** 319, (5-6), 457-459.

12. Iijima, S.; Ichihashi, T., Single-Shell Carbon Nanotubes of 1-Nm Diameter. *Nature* **1993,** 363, (6430), 603-605.

13. Thess, A.; Lee, R.; Nikolaev, P.; Dai, H. J.; Petit, P.; Robert, J.; Xu, C. H.; Lee, Y. H.; Kim, S. G.; Rinzler, A. G.; Colbert, D. T.; Scuseria, G. E.; Tomanek, D.; Fischer, J. E.; Smalley, R. E., Crystalline ropes of metallic carbon nanotubes. *Science* **1996,** 273, (5274), 483-487.

14. Cassell, A. M.; Raymakers, J. A.; Kong, J.; Dai, H. J., Large scale CVD synthesis of single-walled carbon nanotubes. *J. Phys. Chem. B* **1999,** 103, (31), 6484-6492.

15. Deheer, W. A.; Ugarte, D., Carbon Onions Produced by Heat-Treatment of Carbon Soot and Their Relation to the 217.5 Nm Interstellar Absorption Feature. *Chem. Phys. Lett.* **1993,** 207, (4-6), 480-486.

16. Ugarte, D., Curling and Closure of Graphitic Networks under Electron-Beam Irradiation. *Nature* **1992,** 359, (6397), 707-709.

17. Banhart, F.; Fuller, T.; Redlich, P.; Ajayan, P. M., The formation, annealing and self-compression of carbon onions under electron irradiation. *Chem. Phys. Lett.* **1997,** 269, (3-4), 349-355.

18. Ugarte, D., Formation Mechanism of Quasi-Spherical Carbon Particles Induced by Electron-Bombardment. *Chem. Phys. Lett.* **1993,** 207, (4-6), 473-479.

19. Kuznetsov, V. L.; Chuvilin, A. L.; Butenko, Y. V.; Malkov, I. Y.; Titov, V. M., Onion-Like Carbon from Ultra-Disperse Diamond. *Chem. Phys. Lett.* **1994,** 222, (4), 343-348.

20. Cabioc'h, T.; Thune, E.; Riviere, J. P.; Camelio, S.; Girard, J. C.; Guerin, P.; Jaouen, M.; Henrard, L.; Lambin, P., Structure and properties of carbon onion layers deposited onto various substrates. *J. Appl. Phys.* **2002,** 91, (3), 1560-1567.

21. Chen, X. H.; Deng, F. M.; Wang, J. X.; Yang, H. S.; Wu, G. T.; Zhang, X. B.; Peng, J. C.; Li, W. Z., New method of carbon onion growth by radio-frequency plasma-enhanced chemical vapor deposition. *Chem. Phys. Lett.* **2001,** 336, (3-4), 201-204.

22. Sano, N.; Wang, H.; Chhowalla, M.; Alexandrou, I.; Amaratunga, G. A. J., Nanotechnology - Synthesis of carbon 'onions' in water. *Nature* **2001,** 414, (6863), 506-507.

23. Palkar, A.; Melin, F.; Cardona, C. M.; Elliott, B.; Naskar, A. K.; Edie, D. D.; Kumbhar, A.; Echegoyen, L., Reactivity Differences between Carbon Nano Onions (CNOs) Prepared by Different Methods. *Chemistry - An Asian Journal* **2007,** 0, (0), 0.

24. Bacsa, W. S.; Deheer, W. A.; Ugarte, D.; Chatelain, A., Raman-Spectroscopy of Closed-Shell Carbon Particles. *Chem Phys Lett* **1993,** 211, (4-5), 346-352.

25. Rettenbacher, A. S.; Elliott, B.; Hudson, J. S.; Amirkhanian, A.; Echegoyen, L., Preparation and functionalization of multilayer fullerenes (carbon nano-onions). *Chemistry-a European Journal* **2005,** 12, (2), 376-387.

26. Wiley, W. C.; Mclaren, I. H., Time-of-Flight Mass Spectrometer with Improved Resolution. *Rev. Sci. Instrum.* **1955,** 26, (12), 1150-1157.

27. Cornett, D. S.; Amster, I. J.; Duncan, M. A.; Rao, A. M.; Eklund, P. C., Laser Desorption Mass-Spectrometry of Photopolymerized C-60 Films. *J. Phys. Chem.* **1993,** 97, (19), 5036-5039.

28. Kroto, H. W., Carbon Allotropes - Carbon Onions Introduce New Flavor to Fullerene Studies. *Nature* **1992,** 359, (6397), 670-671.

29. Ponomareva, I. V.; Chernozatonskii, L. A., How can carbon onion transform into diamond-like structure. *Microelectron. Eng.* **2003,** 69, (2-4), 625-628.

Table 4.1. Masses of carbon onions and individual layers from one layer to 30 layers.

Number of layers	Number of atoms in layer	Mass of atoms in layer	Total mass of carbon onion
1	60	720	720
2	240	2880	3600
3	540	6480	10080
4	960	11520	21600
5	1500	18000	39600
6	2160	25920	65520
7	2940	35280	100800
8	3840	46080	146880
9	4860	58320	205200
10	6000	72000	277200
11	7260	87120	364320
12	8640	103680	468000
13	10140	121680	589680
14	11760	141120	730800
15	13500	162000	892800
16	15360	184320	1077120
17	17340	208080	1285200
18	19440	233280	1518480
19	21660	259920	1778400
20	24000	288000	2066400

21	26460	317520	2383920
22	29040	348480	2732400
23	31740	380880	3113280
24	34560	414720	3528000
25	37500	450000	3978000
26	40560	486720	4464720
27	43740	524880	4989600
28	47040	564480	5554080
29	50460	605520	6159600
30	54000	648000	6807600

FIGURES

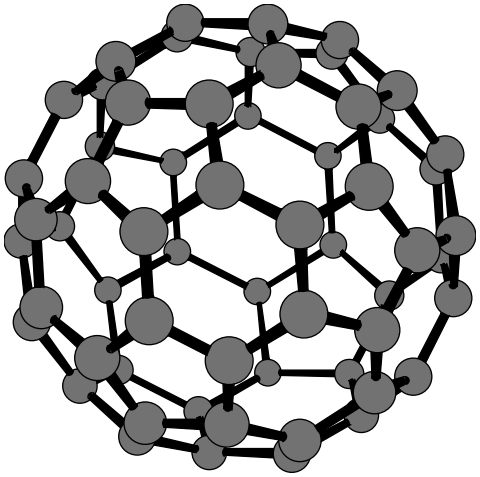

Figure 4.1. Depiction of a C_{60} molecule.

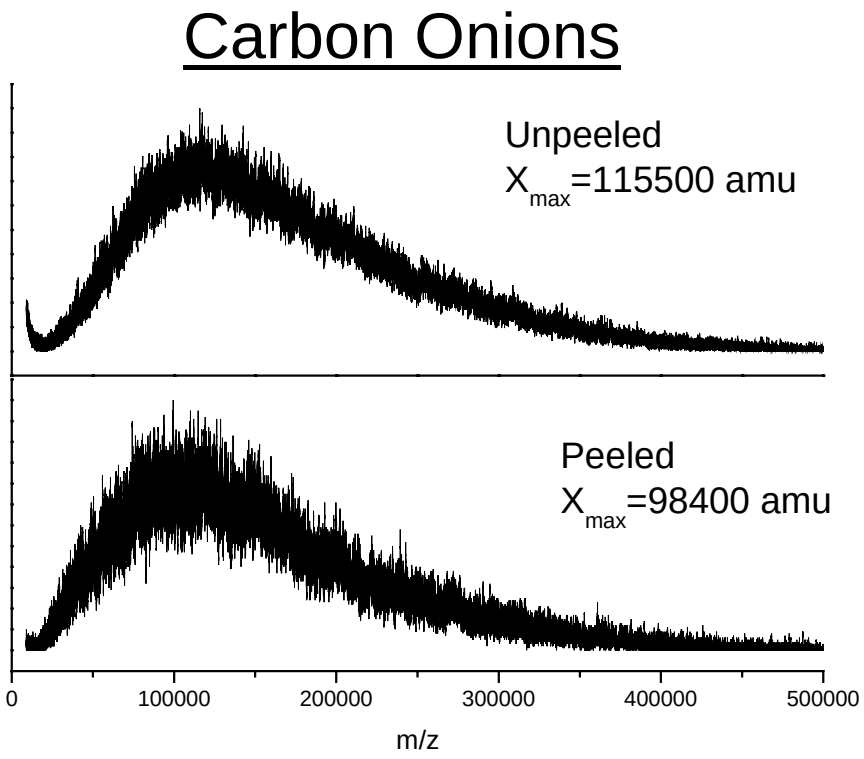

Figure 4.2. Mass spectra for peeled and unpeeled carbon onions.

CHAPTER 5

CONCLUSIONS

5 CONCLUSIONS

Gas phase experiments were carried out on metal sulfur and carbon onion systems. These experiments provided new data about each of these systems. The metal sulfur experiments demonstrated that the $Al_3S_1^+$ cluster is very stable and may even undergo reactions with S_8 in the plasma to produce $Al_3S_9^+$. $Al_3S_9^+$ and larger clusters may undergo a reaction in the plasma with Al_2S_3 to form even larger clusters. Indium sulfur forms many clusters that satisfy Wade's electron counting rules. Gallium is a combined case of aluminum and indium. It forms fewer Wade's rules clusters than indium, and may not add Ga_2S_3 sequentially. Future experiments can be done to verify and go beyond these data. Metal sulfur experiments can be done with photodissociation spectroscopy to determine their structures. Theoretical calculations can also be performed to elucidate structural information. The clusters determined to be stable can also be evaluated for their optical, electrical, and physical properties.

Mass spectrometry studies of carbon onions suggest that the onions formed by an arc discharge in water and by the annealing of nanodiamonds are not monodisperse. Rather, they exhibit a large distribution of masses and sizes. Also, these experiments suggest that there may be many defects in the layers of the carbon onions because such a smooth distribution of masses was observed. There were no magic numbers. Furthermore, the supposedly size-specific synthesis methods need to be evaluated more carefully to determine if they do indeed preferentially form certain sized carbon onions. The data also suggest that the experiments to remove a layer from carbon onions were at least partially successful. More analysis is needed to determine if multiple reactions can remove an entire layer and more than one layer. If they do and specific sizes can be isolated, then size-dependent properties of the properties of carbon onions could be evaluated.